To the Graduate Council:

I am submitting herewith a dissertation written by Chi-Chau Feng entitled "Analysis of Eddy Current Flowmeters." I recommend that it be accepted in partial fulfillment of the requirements for the degree of Doctor of Philosophy, with a major in Physics.

W. E. Deeds

William E. Deeds,
Major Professor

We have read this dissertation
and recommend its acceptance:

Harold C. Schweinler

Cairs V Dodd

H T Matthews

Ro W. Lide

Accepted for the Council:

Hilton A. Smith

Vice Chancellor
Graduate Studies and Research

Thesis
756
.F453
cop. 2

ANALYSIS OF EDDY CURRENT FLOWMETERS

A Dissertation

Presented for the

Doctor of Philosophy

Degree

The University of Tennessee

Chi-Chau Feng

June 1975

1227558

ACKNOWLEDGMENT

The author wishes to express his sincere appreciation to Dr. William E. Deeds, Dr. Caius V. Dodd and the other members of his committee for their patience and many suggestions and guidance during the course of this investigation. He also would like to express his thanks to Dr. W. A. Simpson of the Oak Ridge National Laboratory for his aid during the course of this work, Mr. L. D. Chitwood for helping with the measurements and Mr. Paul Godsey for constructing the coils.

The author was privileged to be able to perform his experiment at the Oak Ridge National Laboratory. Finally, the author wishes to express his thanks to his wife for her patience and encouragement during his tenure in graduate school.

ABSTRACT

Coils can induce and detect eddy currents in nearby conductors. If the conductor is moving, the eddy currents are carried along with it slightly, and properly designed coils can measure the velocity of the moving conductor with considerable accuracy. A general differential equation for the vector potential produced by a sinusoidal current of finite cross section in a moving, conducting medium has been derived. Calculations have been made for various axially symmetric arrangements of coils and conductors using a relaxation program for a computer. Experiments have also been made, using mercury as the flowing conductor, with three- and five-coil flowmeters, with good agreement between measured and computed values. For any given arrangement, there is an optimum frequency of operation, and different frequencies can give information about the velocity distribution.

TABLE OF CONTENTS

CHAPTER		PAGE
1.	INTRODUCTION	1
2.	GENERAL THEORY	5
	Maxwell's Equations for Moving Medium	5
	The Differential Equation for the Vector Potential in a Moving Medium	10
	A Coil Encircling a Hollow Tube	12
3.	RELAXATION METHOD AND COMPUTER PROGRAM	16
	Solution of the General Differential Equation	16
	Adaptation for Computer.	20
	Mutual Impedance and Self Impedance	23
4.	OPTIMIZATION OF THREE-COIL SYSTEM AND FIVE-COIL SYSTEM	25
	Three-Coil System	25
	Five-Coil System	29
	Optimum Distance and Optimum Position	37
5.	EXPERIMENT	49
	Five-Coil System Probe Tube	49
	Three-Coil System Probe Tube	60
	Discussion of Errors	63

CHAPTER PAGE

6. CONCLUSIONS 65

BIBLIOGRAPHY 66

APPENDIXES 69

A 70

B 77

C 79

D 81

VITA 85

LIST OF FIGURES

FIGURE		PAGE
1.	A Coil Encircling a Tube, Through Which a Liquid Metal is Flowing	13
2.	Layout of Problem on a Lattice of Points	19
3.	Diagram of Three-Coil Flowmeter Arrangement	26
4.	Directions and Connections of Winding of the Three-Coil System	27
5.	Diagram of Five-Coil Flowmeter Arrangement	30
6.	Directions and Connections of Winding of the Five-Coil System	31
7.	Five-Coil System, Triple Driver	32
8.	Three-Coil System, Single Driver	33
9.	Layout of the Single Layer, Five-Coil System on a Lattice of Points	38
10.	Optimum Driver Coil Separation	39
11.	Optimum Pickup Coil Position	41
12.	Equivalent Circuit for the Five-Coil System	42
13.	Configuration of Single Layer, Double Layer and Triple Layer Coils	46

FIGURE PAGE

14. Pickup Voltage as a Function of Operating Frequency 47
15. Diagram of Double Layer Five-Coil System 48
16. Diagram of the Experimental Apparatus 50
17. Some Possible Velocity Distributions 52
18. Measured Values and Calculated Values at the Frequency of 5×10^3 Cycles Per Second . . 53
19. Measured Values and Calculated Values at the Frequency of 10^4 Cycles Per Second 54
20. Measured Values and Calculated Values at the Frequency of 2×10^4 Cycles Per Second . . 55
21. Measured Values and Calculated Values at the Frequency of 5×10^4 Cycles Per Second . . 56
22. Measured Values and Calculated Values at the Frequency of 10^5 Cycles Per Second 57
23. Calculated and Measured Slopes for Various Velocity Distributions 59
24. Diagram of the Existing Three-Coil System 61
25. Comparison of the Calculated and Measured Induced Voltage of Three-Coil System Probe Tube at the Frequency of 100 KHz 62
26. The Layout of the Double Layer Five-Coil System on a Lattice of Points 84

CHAPTER 1

INTRODUCTION

In a liquid metal fast breeder reactor, liquid metal is used to cool the core and to transfer its heat to the steam generating plant and turbine. The core must have a guaranteed supply of liquid metal coolant to match the reactor power to the load demand and for safe operation as well. Therefore precise flow measurement of the liquid metal coolant is very important. During reactor operation, these measurements would provide the earliest warning of flow blockage, thereby initiating reactor shutdown before major damage could occur. This thesis, based on eddy current theory and the relaxation method, presents a method for finding the velocity of a moving metal by solving the differential equation for vector potential. To a good approximation, the velocity of the metal is linearly proportional to the difference of the vector potential at two separated pickup coils.

The development of eddy current theory on testing materials can be traced back to 1879. In that year D. E. Hughes (1) used a pair of identical coils to sort materials. In 1952 Förster (2) and his co-workers analyzed a coil above

a conducting plane, assuming the coil to be a magnetic dipole, and also an infinitely long solenoid containing a conducting core. Waidelich and Renken (3) used the method of images to obtain the variation of the impedance of a probe coil near the surface of a metal. Their results for high frequencies were in relatively good agreement with experimental values. Hochschild (4) gave a theoretical analysis of eddy current distribution in the metal and of an infinitely long solenoid. Dodd and Deeds (5) and Dodd (6) gave a relaxation theory to calculate the vector potential of a coil with a finite cross section. Dodd and Deeds (7) used the relaxation method to calculate the electromagnetic forces in conductors. The computed and measured values agree quite well. Dodd and Deeds (8) obtained analytical solutions for axially symmetric eddy-current problems in two configurations. One solution is for a coil above a semi-infinite conducting slab with a plane surface. The other solution is for a coil surrounding an infinitely long circular conducting rod with a uniformly thick coating of another conductor. In both cases, the agreement between the calculated and experimental values is excellent. Tunstall and Dodd (9) gave a computer program to solve eddy-current problems by the relaxation method. Libby and Jenson (10) made a comparison of inside-channel eddy current flowmeters and inside-channel eddy current-ultrasonic flowmeters,

indicating that eddy current flowmeter is most suitable for the proposed application in the FTR subassemblies. Klyuev, Faingoiz and Kapelin (11) gave a theoretical analysis of the movement of a current-conducting plate parallel to the plane of a square transducer. Sheff and Lessor (12) presented a differential equation for vector potential including a velocity term, and they pointed out that, it is this term that gives the effect of interest in a flowmeter.

This thesis extends the relaxation method and the computer program which was given by Tunstall and Dodd and applied it to solve the differential equation for vector potential of coils encircling a hollow tube through which the liquid metal is flowing. Due to axial symmetry, the whole space can be represented by a two dimensional lattice of points. Each point (r,z) has a specified value of current $I(r,z)$, permeability $\mu(r,z)$, conductivity $\sigma(r,z)$ and velocity $u(r,z)$. The vector potential at each point can be solved for any particular configuration of coils, materials and any velocity distribution.

Several three-coil systems (one driver coil and two pickup coils) and five-coil systems (three driver coils and two pickup coils) have been calculated at various frequencies. Comparatively, the five-coil system yields a better result. In order to have an optimum design of flowmeter, various

distances between the driver coils and positions of pickup coils have also been calculated.

Experiments have been performed for both three-coil systems and five-coil systems. The agreement between calculated and measured values is good.

CHAPTER 2

GENERAL THEORY

The differential equations for the vector potential in a moving medium will be derived from Maxwell's equations.

Maxwell's Equations for Moving Medium

Maxwell's equations for stationary media can be written in the form (13)

$$\nabla\cdot\vec{E} = \frac{\rho_{true} - \nabla\cdot\vec{p}}{\varepsilon_o} , \tag{2.1}$$

$$\nabla\cdot\vec{B} = 0 , \tag{2.2}$$

$$\nabla\times\vec{E} = -\frac{\partial\vec{B}}{\partial t} , \tag{2.3}$$

$$\nabla\times\vec{B} = \mu_o(\vec{J}_{true} + \frac{\partial\vec{p}}{\partial t} + \nabla\times M + \varepsilon_o \frac{\partial\vec{E}}{\partial t}) . \tag{2.4}$$

If the medium is moving with a velocity $\vec{u}$, the quantities appearing in Maxwell's equations will be affected by the motion of the medium. Panofsky and Phillips pointed out that, if $\vec{u}$ is small compared to the velocity of light, the first and the second equations are not affected by this motion, since nonrelativistically the charge density of the medium is not affected by the state of motion of the observer. Let us consider the third equation. We can write the

following derivation:

$$\frac{d\vec{B}}{dt} = \frac{\partial \vec{B}}{\partial t} + (\vec{u}\cdot\nabla)\ \vec{B} \ . \tag{2.5}$$

By the vector identity

$$\nabla\times(\vec{B}\times\vec{u}) = (\vec{u}\cdot\nabla)\vec{B} - \vec{u}(\nabla\cdot\vec{B}) - (\vec{B}\cdot\nabla)\vec{u} + \vec{B}(\nabla\cdot\vec{u}) \ , \tag{2.6}$$

we have

$$(\vec{u}\cdot\nabla)\vec{B} = \nabla\times(\vec{B}\times\vec{u}) + \vec{u}(\nabla\cdot\vec{B}) + (\vec{B}\cdot\nabla)\vec{u} - \vec{B}(\nabla\cdot\vec{u}) \ , \tag{2.7}$$

Assuming the velocity $\vec{u}$ has only a z-component and is a function of r, and the magnetic induction $\vec{B}$ has only a ϕ-component, then we have

$$\vec{u} = \hat{e}_z u_z(r) \ ,$$

$$\vec{B} = \hat{e}_\phi B_\phi \ ,$$

$$\nabla\cdot\vec{u} = \frac{1}{r}\frac{\partial}{\partial r}(ru_r) + \frac{1}{r}\frac{\partial u_\phi}{\partial \phi} + \frac{\partial u_z(r)}{\partial z}$$

$$= \frac{\partial u_z(r)}{\partial z} = 0 \ ,$$

$$(\vec{B}\cdot\nabla)\vec{u} = B_\phi \frac{1}{r}\frac{\partial}{\partial \phi} u_z(r) = 0 \ ,$$

and

$$\nabla\cdot\vec{B} = 0 \ .$$

Since the last three terms in the r.h.s. of equation (2.7) are zero, then

$$(\vec{u}\cdot\nabla)\vec{B} = \nabla\times(\vec{B}\times\vec{u}) \ ,$$

$$\therefore \frac{d\vec{B}}{dt} = \frac{\partial\vec{B}}{\partial t} + \nabla\times(\vec{B}\times\vec{u}) \ , \qquad (2.8)$$

and

$$\oint E'\cdot d\vec{\ell} = -\frac{d\phi_m}{dt} = -\int[\frac{\partial\vec{B}}{\partial t} + \nabla\times(\vec{B}\times\vec{u})]\cdot d\vec{s} \ . \qquad (2.9)$$

By applying Stokes' theorem, we have

$$\oint(\nabla\times\vec{E}')\cdot d\vec{s} = -\int[\frac{\partial\vec{B}}{\partial t} + \nabla\times(\vec{B}\times\vec{u})]\cdot d\vec{s} \ , \qquad (2.10)$$

$$\nabla\times\vec{E}' = -\frac{\partial\vec{B}}{\partial t} - \nabla\times(\vec{B}\times\vec{u}) \ , \qquad (2.11)$$

where $\vec{E}'$ is the field measured in the moving medium. Equation (2.11) can be written in the form

$$\nabla\times(\vec{E}'-\vec{u}\times\vec{B}) = -\frac{\partial\vec{B}}{\partial t} \ . \qquad (2.12)$$

Let

$$\vec{E} = \vec{E}'-\vec{u}\times\vec{B} \ , \qquad (2.13)$$

$\vec{E}$ is the field that is measured by a stationary observer. Hence, for a stationary observer, equation (2.12) becomes

$$\nabla\times\vec{E} = -\frac{\partial\vec{B}}{\partial t} \ . \qquad (2.14)$$

Therefore the third Maxwell's equation is not affected by the motion of the medium either. The only modification is a correction to the current in the fourth Maxwell's equation. Again from Panofsky and Phillips, the total current which gives rise to the magnetic field is composed of the following parts:

(1) True current $\vec{J}_{true}$,

(2) Convective current $\vec{u}(\rho_{true} - \nabla\cdot\vec{p})$,

(3) Current caused by the rate of change of the polarization and the motion of polarized media, given by $\frac{d\vec{p}}{dt} = \frac{\partial\vec{p}}{\partial t} + \nabla\times(\vec{p}\times\vec{u}) + (\nabla\cdot\vec{p})\vec{u}$,

(4) Vacuum displacement current $\varepsilon_o\frac{\partial\vec{E}}{\partial t}$,

(5) Magnetization current* $\vec{J}_m = \nabla\times\vec{M}$,

with these corrections to the fourth of Maxwell's equations, we have

$$\nabla\times\vec{B} = \mu_o\left[\vec{J}_{true} + \vec{u}(\rho_{true} - \nabla\cdot\vec{p}) + \nabla\times\vec{M} + \frac{\partial\vec{p}}{\partial t} + \nabla\times(\vec{p}\times\vec{u}) + (\nabla\cdot\vec{p})\,\vec{u} + \varepsilon_o\frac{\partial\vec{E}}{\partial t}\right]$$

$$= \mu_o\left[\vec{J}_{true} + \rho_{true}\vec{u} + \nabla\times\vec{M} + \frac{\partial\vec{p}}{\partial t} + \nabla\times(\vec{p}\times\vec{u}) + \varepsilon_o\frac{\partial\vec{E}}{\partial t}\right] ,$$

$$\nabla\times\left(\frac{\vec{B}}{\mu_o} - \vec{M}\right) = \vec{J}_{true} + \rho_{true}\vec{u} + \frac{\partial\vec{p}}{\partial t} + \nabla\times(\vec{p}\times\vec{u}) + \varepsilon_o\frac{\partial\vec{E}}{\partial t} \quad . (2.15)$$

---

*Panofsky and Phillips did not have this term in their derivation for a nonmagnetized medium.

Since $\vec{H} = \frac{\vec{B}}{\mu_o} - \vec{M}$, (2.16)

therefore we have

$$\nabla\times\vec{H} = \vec{J}_{true}' + \rho_{true}\,\vec{u} + \frac{\partial\vec{p}}{\partial t} + \nabla\times(\vec{p}\times\vec{u}) + \varepsilon_o\frac{\partial\vec{E}}{\partial t} . \qquad (2.17)$$

Now we can write the Maxwell's equations in a medium moving with a velocity $\vec{u}$ which is small compared with the velocity of light as follows:

$$\nabla\cdot\vec{E} = \frac{1}{\varepsilon_o}(\rho_{true} - \nabla\cdot\vec{p}) \qquad (2.18)$$

$$\nabla\cdot B = 0 , \qquad (2.19)$$

$$\nabla\cdot\vec{E} = -\frac{\partial\vec{B}}{\partial t} , \qquad (2.20)$$

$$\nabla\times\vec{H} = \vec{J}_{true} + \rho_{true}\vec{u} + \frac{\partial\vec{p}}{\partial t} + \nabla\times(\vec{p}\times\vec{u}) + \varepsilon_o\frac{\partial\vec{E}}{\partial t} , \qquad (2.21)$$

with

$$\vec{J}_{true} = \sigma\vec{E}' = \sigma(\vec{E}+\vec{u}\times\vec{B}) , \qquad (2.22)$$

$$\vec{P} = \varepsilon_o(\kappa-1)(\vec{E}+\vec{u}\times\vec{B}) . \qquad (2.23)$$

If the medium is taken to be a metal or air, uncharged, inhomogeneous, linear, and isotropic, then the polarization $\vec{P}$ would be zero and

$\vec{B} = \mu\vec{H}$. With (2.24)

$\vec{J}_{true} = \sigma(\vec{E}+\vec{u}\times\vec{B})$ substituted into equation (2.21), the Maxwell's equations can be written as

$$\nabla\times\vec{E} = 0 \ , \tag{2.25}$$

$$\nabla\cdot\vec{B} = 0 \ , \tag{2.26}$$

$$\nabla\times\vec{E} = -\frac{\partial\vec{B}}{\partial t} \ , \tag{2.27}$$

$$\nabla\times\frac{\vec{B}}{\mu} = \sigma\vec{E} + c(\vec{u}\times\vec{B}) + \varepsilon_o\frac{\partial\vec{E}}{\partial t} \ . \tag{2.28}$$

The Differential Equation for the Vector Potential in a Moving Medium

Since the term $\sigma\vec{E} >> \varepsilon_o \frac{\partial\vec{E}}{\partial t}$ for reasonable conductors at frequencies below about 10 megacycles per second (7), the latter may be neglected at low frequencies. The magnetic induction $\vec{B}$ may be expressed as the curl of a vector potential $\vec{A}$: $\vec{B} = \nabla\times\vec{A}$.

Substituting this into equation (2.27), gives

$$\nabla\times\vec{E} = -\frac{\partial}{\partial t}\nabla\times\vec{A} = -\nabla\times\frac{\partial\vec{A}}{\partial t} \ ,$$

$$\nabla\times(\vec{E}+\frac{\partial\vec{A}}{\partial t}) = 0 \ , \tag{2.29}$$

or

$$\vec{E} = -\frac{\partial\vec{A}}{\partial t} - \nabla\psi \ ,$$

$$\sigma\vec{E} = -\sigma\frac{\partial\vec{A}}{\partial t} - \sigma\nabla\psi \ , \tag{2.30}$$

where ψ is a scalar potential.

We can set limit $(-\sigma\nabla\psi) = \vec{J}_o$, (6) (2.31)

$\sigma \to o$.

$\nabla\psi \to \infty$.

where $\vec{J}_o$ is the amplitude of an alternating current density. Equation (2.30) then becomes

$$\sigma\vec{E} = -\sigma\frac{\partial\vec{A}}{\partial t} + \vec{J}_o \ . \tag{2.32}$$

Substituting equation (2.32) into the right hand side of equation (2.28) and neglecting the last term, we have

$$\nabla\times\frac{\vec{B}}{\mu} = \vec{J}_o - \sigma\frac{\partial\vec{A}}{\partial t} + \sigma(\vec{u}\times\vec{B}) . \tag{2.33}$$

The first term on the left hand side can be rewritten by use of the vector identities:

$$\nabla\times(\psi\vec{F}) = (\nabla\psi)\times\vec{F} + \psi\nabla\times\vec{F} \quad \text{and}$$

$$\nabla\times(\nabla\times\vec{F}) = \nabla(\nabla\cdot\vec{F}) - \nabla^2\vec{F} \ , \tag{2.34}$$

$$\begin{aligned}\nabla\times\frac{\vec{B}}{\mu} &= \nabla(\frac{1}{\mu})\times\vec{B} + \frac{1}{\mu}\nabla\times\vec{B} \\ &= \nabla(\frac{1}{\mu})\times(\nabla\times\vec{A}) + \frac{1}{\mu}\nabla\times(\nabla\times\vec{A}) \\ &= \nabla(\frac{1}{\mu})\times(\nabla\times\vec{A}) + \frac{1}{\mu}\nabla(\nabla\cdot\vec{A}) - \frac{1}{\mu}\nabla^2\vec{A} \ .\end{aligned} \tag{2.35}$$

If we use the Coulomb gauge ($\nabla\cdot\vec{A} = 0$), in our induction problem, then equation (2.33) can be written as

$$\nabla^2\vec{A} = -\mu\vec{J}_o + \mu\sigma\frac{\partial\vec{A}}{\partial t} - \mu\sigma(\vec{u}\times(\nabla\times\vec{A})) + \mu\nabla(\frac{1}{\mu})\times(\nabla\times\vec{A}) \ . \tag{2.36}$$

This is the equation for the vector potential in an isotropic linear, inhomogeneous medium, moving with velocity $\vec{u}$ relative to the measuring system.

A Coil Encircling a Hollow Tube

The problem of a coil encircling a hollow tube, through which a liquid metal is flowing with only axial flow components is shown in Figure 1. The driving current $\vec{J}_o$ and vector potential $\vec{A}$ each have only a θ-component:

$$\vec{J}_o = \hat{e}_\theta J_o \qquad \text{and} \qquad \vec{A} = \hat{e}_\theta A \ , \tag{2.37}$$

and the velocity $\vec{u}$ has only a z-component

$$\vec{u} = \hat{e}_z u \ . \tag{2.38}$$

For cylindrical coordinates, the θ-component of $\nabla^2\vec{A}$ is

$$\nabla^2 A_\theta = \frac{\partial^2 A_\theta}{\partial r^2} + \frac{1}{r}\frac{\partial A_\theta}{\partial r} + \frac{\partial^2 A_\theta}{\partial z^2} - \frac{A_\theta}{r^2} \ . \tag{2.39}$$

Also,

$$\nabla\times\vec{A} = \hat{e}_r\left(\frac{1}{r}\frac{\partial A_z}{\partial\theta} - \frac{\partial A_\theta}{\partial z}\right) + \hat{e}_\theta\left(\frac{\partial A_r}{\partial z} - \frac{\partial A_z}{\partial r}\right) + \hat{e}_z\left(\frac{1}{r}\frac{\partial}{\partial r}(rA_\theta) - \frac{1}{r}\frac{\partial A_r}{\partial\theta}\right)$$

$$= -\hat{e}_r\frac{\partial A_\theta}{\partial z} + \hat{e}_z\frac{1}{r}\frac{\partial}{\partial r}(rA_\theta) \ , \tag{2.40}$$

so that

$$\vec{u}\times(\nabla\times\vec{A}) = \hat{e}_z u\times\left[-\hat{e}_r\frac{\partial A_\theta}{\partial z} + \hat{e}_z\frac{1}{r}\frac{\partial}{\partial r}(rA_\theta)\right]$$

$$= -\hat{e}_\theta u\frac{\partial A_\theta}{\partial z} \ , \tag{2.41}$$

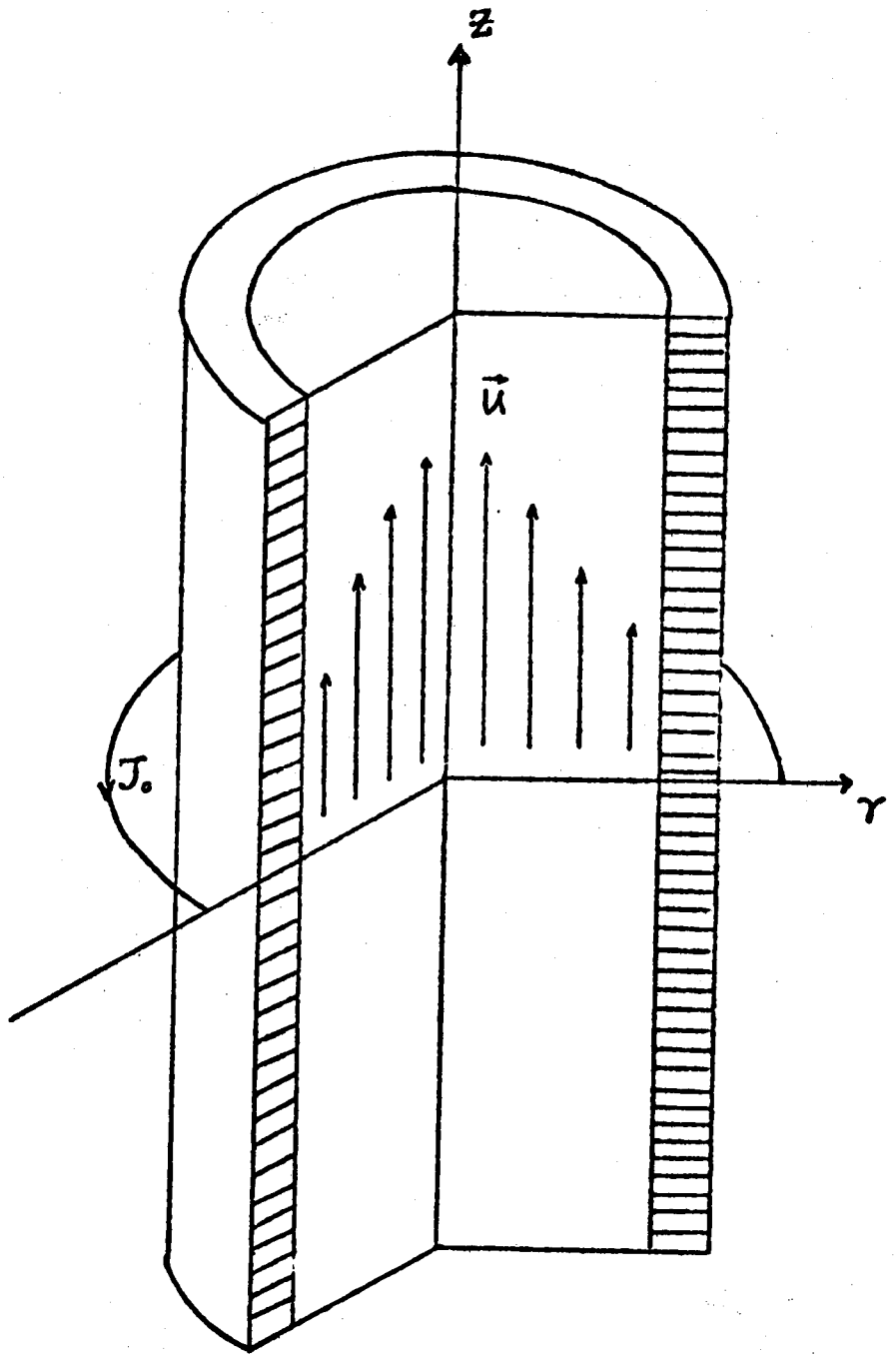


Figure 1. A coil encircling a tube, through which a liquid metal is flowing.

and

$$\nabla\left(\frac{1}{\mu}\right) = \hat{e}_r\left(\frac{\partial\left(\frac{1}{\mu}\right)}{\partial r}\right) + \hat{e}_\theta\frac{1}{r}\left(\frac{\partial\left(\frac{1}{\mu}\right)}{\partial\theta}\right) + \hat{e}_z\left(\frac{\partial\left(\frac{1}{\mu}\right)}{\partial z}\right), \qquad (2.42)$$

so that

$$\nabla\left(\frac{1}{\mu}\right)\times(\nabla\times\vec{A}) = \left[\hat{e}_r\left(\frac{\partial\left(\frac{1}{\mu}\right)}{\partial r}\right) + \hat{e}_\theta\frac{1}{r}\left(\frac{\partial\left(\frac{1}{\mu}\right)}{\partial\theta}\right) + \hat{e}_z\left(\frac{\partial\left(\frac{1}{\mu}\right)}{\partial z}\right)\right]$$

$$\times\left[-\hat{e}_r\frac{\partial A_\theta}{\partial z} + \hat{e}_z\frac{1}{r}\frac{\partial(rA_\theta)}{\partial r}\right]$$

$$= -\hat{e}_r\frac{1}{r}2\left(\frac{\partial\left(\frac{1}{\mu}\right)}{\partial\theta}\right)\left(\frac{\partial(rA_\theta)}{\partial r}\right)$$

$$-\hat{e}_\theta\left[\left(\frac{\partial\left(\frac{1}{\mu}\right)}{\partial r}\right)\left(\frac{1}{r}\frac{\partial(rA_\theta)}{\partial r}\right) + \left(\frac{\partial\left(\frac{1}{\mu}\right)}{\partial z}\right)\left(\frac{\partial A_\theta}{\partial z}\right)\right]$$

$$+\hat{e}_z\frac{1}{r}\left(\frac{\partial\left(\frac{1}{\mu}\right)}{\partial\theta}\right)\left(\frac{\partial A_\theta}{\partial z}\right). \qquad (2.43)$$

Substituting equations (2.37), (2.39), (2.41), and the θ-component of equation (2.43) into equation (2.36), we can write the equation for A_θ as

$$\frac{\partial^2 A_\theta}{\partial r^2} + \frac{1}{r}\frac{\partial A_\theta}{\partial r} + \frac{\partial^2 A_\theta}{\partial z^2} - \frac{A_\theta}{r^2} = -\mu J_o + \mu\sigma\frac{\partial A_\theta}{\partial t} + \mu\sigma u\frac{\partial A_\theta}{\partial z}$$

$$-\mu\left[\frac{\partial\left(\frac{1}{\mu}\right)}{\partial r}\left(\frac{1}{r}\frac{\partial(rA_\theta)}{\partial r}\right) + \left(\frac{\partial\left(\frac{1}{\mu}\right)}{\partial z}\right)\frac{\partial A_\theta}{\partial z}\right] \qquad (2.44)$$

Assuming

$$J_o = J_o' e^{i\omega t}, \qquad \text{and} \qquad A_\theta = A' e^{i\omega t},$$

and substituting into equation (2.44), we have

$$\frac{\partial^2 A'}{\partial r^2} e^{i\omega t} + \frac{1}{r}\frac{\partial A'}{\partial r} e^{i\omega t} + \frac{\partial^2 A'}{\partial z^2} e^{i\omega t} - \frac{A'}{r^2} e^{i\omega t} = -J_o' e^{i\omega t}$$

$$+ i\omega\mu\sigma A' e^{i\omega t} + \mu\sigma u \frac{\partial A'}{\partial z} e^{i\omega t} - \mu\left[\frac{\partial(\frac{1}{\mu})}{\partial r}\left(\frac{1}{r}\frac{\partial(rA')}{\partial r} e^{i\omega t}\right)\right.$$

$$\left. + \left(\frac{\partial(\frac{1}{\mu})}{\partial z}\right)\frac{\partial A'}{\partial z} e^{i\omega t}\right].$$

Cancelling out the term $e^{i\omega t}$ and dropping the primes gives

$$\frac{\partial^2 A}{\partial r^2} + \frac{1}{r}\frac{\partial A}{\partial r} + \frac{\partial^2 A}{\partial z^2} - \frac{A}{r^2} = -\mu J_o + i\omega\mu\sigma A + \mu\sigma u\frac{\partial A}{\partial z}$$

$$- \mu\left[\frac{\partial(\frac{1}{\mu})}{\partial r}\left(\frac{1}{r}\left(\frac{\partial(rA)}{\partial r}\right)\right) + \left(\frac{\partial(\frac{1}{\mu})}{\partial z}\right)\frac{\partial A}{\partial z}\right]. \qquad (2.45)$$

This is the general differential equation for the vector potential in a linear, inhomogeneous, moving, conducting medium with a sinusodial driving current. The third term ($\mu\sigma u\frac{\partial A}{\partial z}$) on the right hand side of this equation is the velocity term. It is this term that gives the effect of interest in an eddy-current flowmeter.

CHAPTER 3

RELAXATION METHOD AND COMPUTER PROGRAM

We shall solve the general differential equation

$$\frac{\partial^2 A}{\partial r^2} + \frac{1}{r}\frac{\partial A}{\partial r} + \frac{\partial^2 A}{\partial z^2} - \mu\sigma u\frac{\partial A}{\partial z} - \frac{A}{r^2} - i\omega\mu\sigma A = -\mu J_o$$

$$- \mu\left[\frac{\partial(\frac{1}{\mu})}{\partial r}\left(\frac{1}{r}\frac{\partial(rA)}{\partial r}\right) + \frac{\partial(\frac{1}{\mu})}{\partial z}\frac{\partial A}{\partial z}\right] \qquad (3.1)$$

by the relaxation method using a computer.

Solution of the General Differential Equation

The finite difference equations for various derivatives of the vector potential are (7):

$$\left(\frac{\partial A}{\partial r}\right)_{z,r} = \frac{A_{z,r+h} - A_{z,r}}{h}, \qquad (3.2)$$

$$\left(\frac{\partial^2 A}{\partial r^2}\right)_{z,r} = \frac{A_{z,r+h} + A_{z,r-h} - 2A_{z,r}}{h^2}, \qquad (3.3)$$

$$\left(\frac{\partial A}{\partial z}\right)_{z,r} = \frac{A_{z+h,r} - A_{z,r}}{h}, \qquad (3.4)$$

$$\left(\frac{\partial^2 A}{\partial z^2}\right)_{z,r} = \frac{A_{z+h,r} + A_{z-h,r} - 2A_{z,r}}{h^2}, \qquad (3.5)$$

$$\left(\frac{\partial(\frac{1}{\mu})}{\partial r}\right)_{z,r} = \frac{\frac{1}{\mu_{z,r+h}} - \frac{1}{\mu_{z,r}}}{h} , \tag{3.6}$$

$$\left(\frac{\partial(\frac{1}{\mu})}{\partial z}\right)_{z,r} = \frac{\frac{1}{\mu_{z+h,r}} - \frac{1}{\mu_{z,r}}}{h} . \tag{3.7}$$

$$\left(\frac{1}{r}\frac{\partial(rA)}{\partial r}\right)_{z,r} = \frac{(r+h)A_{z,r+h} - rA_{z,r}}{rh} . \tag{3.8}$$

Substituting equations (3.2) through (3.8) into equation (3.1) and solving for the vector potential at any point $A_{z,r}$ in terms of the vector potential at the four nearest neighboring points, we have

$$A_{z,r} = \left\{(1+\frac{h}{r})(\frac{\mu_{z,r}}{\mu_{z,r+h}})A_{z,r+h} + A_{z,r-h} + \left[\frac{\mu_{z,r}}{\mu_{z+h,r}} - h\mu_{z,r}\sigma_{z,r}u_{z,r}\right]A_{z+h,r} + A_{z-h,r} + h^2\mu_{z,r}J_{z,r}\right\} \div \left\{2+\frac{h}{r} + \frac{h^2}{r^2} - h\mu_{z,r}\sigma_{z,r}u_{z,r} + \frac{\mu_{z,r}}{\mu_{z,r+h}} + \frac{\mu_{z,r}}{\mu_{z+h,r}} + ih^2\omega\mu_{z,r}\sigma_{z,r}\right\} , \tag{3.9}$$

where $\mu_{z,r}$, $J_{z,r}$, $\sigma_{z,r}$, $u_{z,r}$ and ω are respectively the permeability, applied current density, conductivity, velocity and angular frequency at each point z,r. Because of the

axial symmetry, if we make the coordinate z always greater than zero, we need to consider lattice points only in a quarter-plane through the symmetry axis, as shown in Figure 2. Previous experience has shown that, for a reasonable compromise between accuracy and economy, the quarter-plane can be divided into N x M lattice points, where N and M are integers such that $(N-1)h = 6R$ and $(M-1) = 4R$, if R is the mean coil radius and h is the distance between two adjacent lattice points. The coordinates of each point are (z_n, r_m), where $z_n = (n-1)h$, $r_m = (m-1)h$, $n = 1,2,.....N$, $m = 1,2,.....M$. The vector potential at the point (z_n, r_m) in equation (3.9) can be expressed by

$$A_{n,m} = \left[\left(1+\frac{1}{m-1}\right) \left(\frac{\mu_{n,m}}{\mu_{n,m-1}}\right) A_{n,m+1} + A_{n,m-1} + \left(\frac{\mu_{n,m}}{\mu_{n+1,m}} - h\mu_{n,m}\sigma_{n,m}u_{n,m}\right) A_{n+1,m} + A_{n-1,m} + h^2\mu_{n,m}J_{n,m} \right] \div \left[2+\frac{1}{m-1} + \frac{1}{(m-1)^2} - h\mu_{n,m}\sigma_{n,m}u_{n,m} + \frac{\mu_{n,m}}{\mu_{n+1,m}} + \frac{\mu_{n,m}}{\mu_{n+1,m}} + ih^2\omega\mu_{n,m}\sigma_{n,m} \right], \quad (3.10)$$

where $A_{n,m} = A(z_n, r_m)$, $n = 2,3,.....N-1$, $m = 2,3,.....M-1$. The vector potential is zero along the axis and at infinity, but, for practical purposes with the restriction on N and M, we can define $A_{n,m}$ to be zero on the boundaries of the

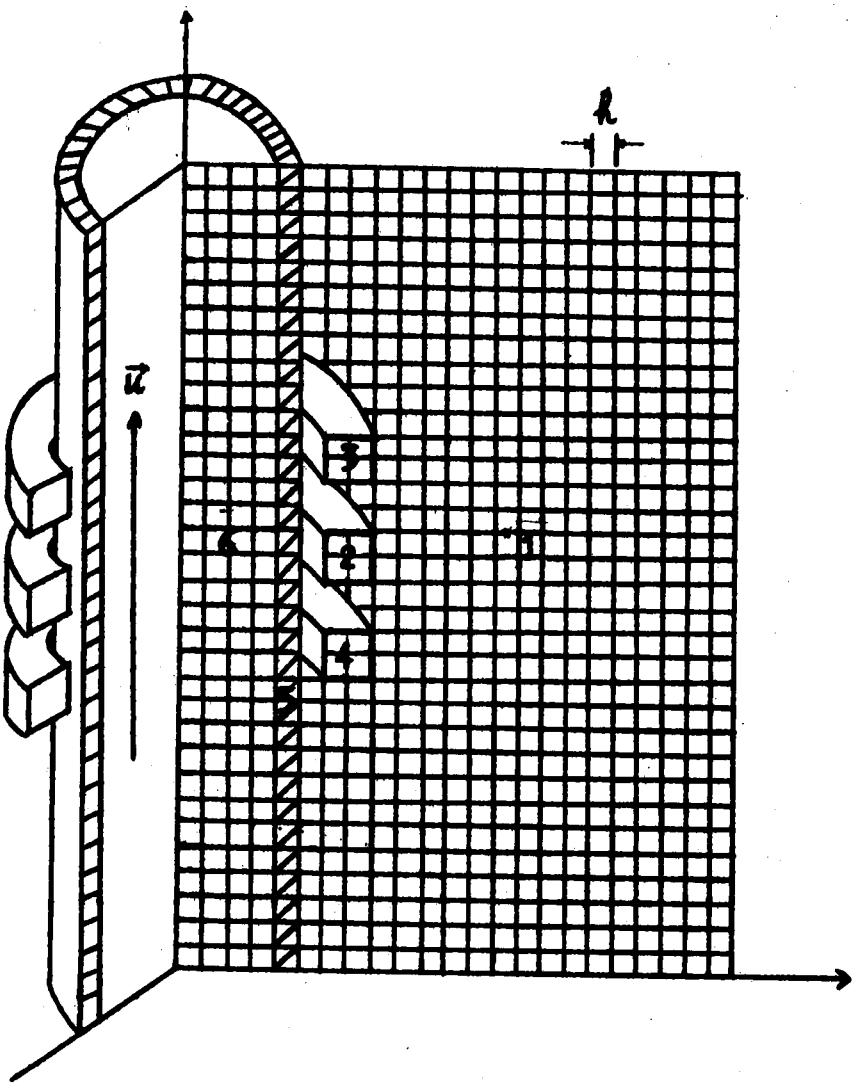


Figure 2. Layout of problem on a lattice of points.

quarter-plane. With these boundary conditions and equation (3.10), we can solve for the vector potential for every point in the quarter-plane. We use a point successive over-relaxation (SOR) iteration technique in which, at the k^{th} iteration (9),

$$A_{n,m}^{(k)} = A_{n,m}^{(k-1)} + W(A_{n,m}^{calc} - A_{n,m}^{(k-1)}) \quad , \tag{3.11}$$

where $k \geq 1$, $0<W<2$, $A_{n,m}^{(k-1)}$ is the value obtained in the $(k-1)^{th}$ iteration, and $A_{n,m}^{calc}$ denotes the calculated value obtained from equation (3.10). If W is not too large, after many iterations the vector potential will converge to a value satisfying Maxwell's equations (within the approximation set by the coarseness of the lattice).

Adaptation for Computer (9)

Equation (3.10) can be simplified depending on the location of the point (z_n, r_m), since many of the terms vanish outside of the point (z_n, r_m), they are:

$\sigma_{n,m} = 0$ if (z_n, r_m) is not in a conductor,

$J_{n,m} = 0$ if (z_n, r_m) is not in the driver coils,

$u_{n,m} = 0$ if (z_n, r_m) is not in the flowing metal.

Taking advantage of these properties, we divide the medium into sections S_K, K = 1,2.....l, l is the number of sections, and assign S_1 to air, S_2 to the driver coil, S_3 to the upper pickup coil, S_4 to the lower pickup coil, S_5 to the

conducting tube, S_6 to the flowing metal, in the example as shown in Figure 2. Each point in the same section has the same values of σ, J, μ, and u. Let us define the following functions:

(1) A point set function $\beta(z_n, r_m)$ by

$$\beta_{n,m} = (z_n, r_m) = K,$$

where K is the index of the point (z_n, r_m) in section S_K;

(2) The relative permeability $\bar{\mu}_K$ by

$$\bar{\mu}_K = \frac{\mu_K}{\mu_o} \tag{3.13}$$

where μ_o is the permeability of free space, and μ_K is the permeability of the point (z_n, r_m) in section S_K;

(3) The function $\alpha(K)$ by

$$\alpha(K) = \begin{cases} 1, & \text{if K is the index of a driver coil,} \\ 0, & \text{otherwise;} \end{cases} \tag{3.14}$$

(4) A function $\theta(K)$ by

$$\theta(K) = \begin{cases} 1, & \text{if K is the index of the flowing metal,} \\ 0, & \text{otherwise;} \end{cases} \tag{3.15}$$

(5) $$\hat{F} = h^2 \omega \mu_{K1} \sigma_{K1} \tag{3.16}$$

and

$$F = (h^2 \omega \mu_{Ki} \sigma_{Ki}) / \hat{F}, \quad i=1,2,....c, \tag{3.17}$$

where c is the number of conducting sections, for example

as shown in Figure 2, c = 2 and $K_1 = 5$, $K_2 = 6$;

(6) A function $\gamma(K)$ by

$$\gamma(K) = \begin{cases} 0, \text{ if K is not the index of a conducting} \\ \text{section,} \\ F_i, \text{ if } K = K_i \text{ for some i, } i = 1,2,....c, \end{cases} \tag{3.18}$$

Using the above function, we can express the vector potential $A_{n,m}$ by

$$A_{n,m} = \left\{ (1+\frac{1}{m-1})\frac{\overline{\mu}_K}{\overline{\mu}_s} A_{n,m+1} + A_{n,m-1} + \left(\frac{\overline{\mu}_K}{\overline{\mu}_t} - h\mu_K\sigma_K u_K \theta(K) \right) A_{m+1,m} \right.$$

$$\left. + A_{n-1,m} + \alpha(K)\overline{\mu}_K \right\} \div \left\{ 2+\frac{1}{m-1} + \frac{1}{(m-1)^2} + \frac{\overline{\mu}_K}{\overline{\mu}_s} + \frac{\overline{\mu}_K}{\overline{\mu}_t} \right.$$

$$\left. - h\mu_K\sigma_K u_K \theta(K) + i\hat{F}\alpha(K) \right\}, \tag{3.19}$$

where $K = \beta_{n,m}$, $S = \beta_{n,m-1}$, $t = \beta_{n+1,m}$.

This is the form of equation which the computer code utilizes (see Appendix).

For the air case, where no conducting materials are present, equation (3.19) becomes

$$\hat{A}_{n,m} = \left\{ (1+\frac{1}{m-1})\frac{\overline{\mu}_K}{\overline{\mu}_s} \hat{A}_{n,m+1} + \hat{A}_{n,m-1} + \frac{\overline{\mu}_K}{\overline{\mu}_t} \hat{A}_{n+1,m} + \hat{A}_{n-1,m} \right.$$

$$+ \alpha(K)\bar{\mu}_K \Big\} \div \left\{ 2 + \frac{1}{m-1} + \frac{1}{(m-1)^2} + \frac{\bar{\mu}_K}{\bar{\mu}_s} + \frac{\bar{\mu}_K}{\bar{\mu}_t} \right\} , \qquad (3.20)$$

where $\hat{A}_{n,m}$ is a real-valued quantity.

Note that the last term $h^2\mu_{n,m}J_{n,m}$ in the numerator of equation (3.10) is replaced by $\alpha(K)\bar{\mu}_K$, in equation (3.19). This sets

$$\bar{\mu}_K = h^2\mu_K J_K .$$

Therefore we have

$$J_K = \frac{\bar{\mu}_K}{\mu_K h^2} + \frac{1}{\mu_o h^2} . \qquad (3.21)$$

The current in one turn of wire would be

$$I = h^2 J_K = \frac{N}{n\mu_o} , \qquad (3.22)$$

where N is the number of lattice points in the driver coil and n is the number of turns of wire in the driver coil.

Mutual Impedance and Self Impedance

Once the vector potential has been determined, any physically observable electromagnetic quantity can be calculated from it. We shall now derive the mutual impedance between the driver coil and the pickup coil, and the self-impedance of the driver coil.

The voltage induced in a length of wire in the oscillating field is (8)

$$V = i\omega \int \vec{A} \cdot d\vec{s}. \tag{3.23}$$

For a pickup coil containing N′ lattice points at radius r, equation (3.23) becomes

$$V = i\omega \sum_{N'} 2\pi r A_{n,m}. \tag{3.24}$$

Substituting r=h(m-1) into equation (3.24), we have

$$V = i\omega h \sum_{N'} 2\pi (m-1) A_{n,m}. \tag{3.25}$$

Suppose there are actually n′ turns of wire in the pickup coil, then each point would have n′/N′ turns of wire. The induced voltage in the pickup coil would then be

$$V = i\omega \frac{n'}{N'} \sum_{N'} 2\pi (m-1) A_{n,m}. \tag{3.26}$$

Thus the mutual impedance is given by

$$M = \frac{V}{I}$$

$$= \frac{i\omega \frac{n'}{N'} h \sum_{N'} 2\pi (m-1) A_{n,m}}{\frac{N}{n\mu_o}}$$

$$= i\omega \left(\frac{n'}{N'}\right) \left(\frac{n}{N}\right) h\mu_o \sum_{N'} 2\pi (m-1) A_{n,m}. \tag{3.27}$$

Similarly the self impedance is given by

$$Z = i\omega \left(\frac{n'}{N'}\right)^2 h\mu_o \sum_{N'} 2\pi (m-1) A_{n,m}. \tag{3.28}$$

CHAPTER 4

OPTIMIZATION OF THREE-COIL SYSTEM AND FIVE-COIL SYSTEM

Three-Coil System

The three-coil system consists of a driver coil and two pickup coils encircling a tube, which may or may not be conducting, the flowing conductor in the center is assumed to have only axial flow components along the z-axis. Figure 3 is the cutaway drawing of the system, coil 5 is the driver coil, and coil 3 and coil 4 are the pickup coils. The directions of winding and their connections are shown in Figure 4. The wire in the pickup coils are connected in series, but in opposite directions. All coils have axial symmetry, and pickup coil 3 and 4 are identical and symmetrically located with respect to the central driver coil.

We shall calculate the induced voltages at the pickup coils. By equation (3.27), the mutual impedance between coil 3 and coil 5 is given by

$$M_{35} = i\omega\left(\frac{n'}{N}\right)\left(\frac{n}{N}\right)h\mu_o \sum_{\text{coil } 3} 2\pi(m-1)A_{n,m} , \qquad (4.1)$$

and the mutual impedance between coil 4 and coil 5 is given by

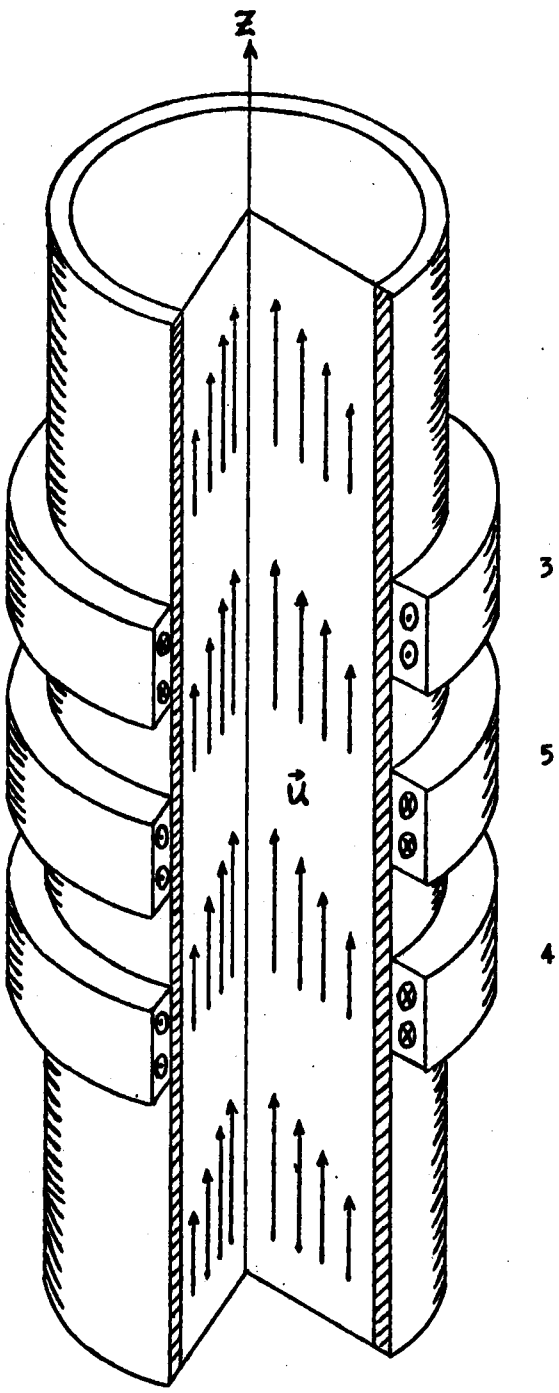


Figure 3. Diagram of three-coil flowmeter arrangement.

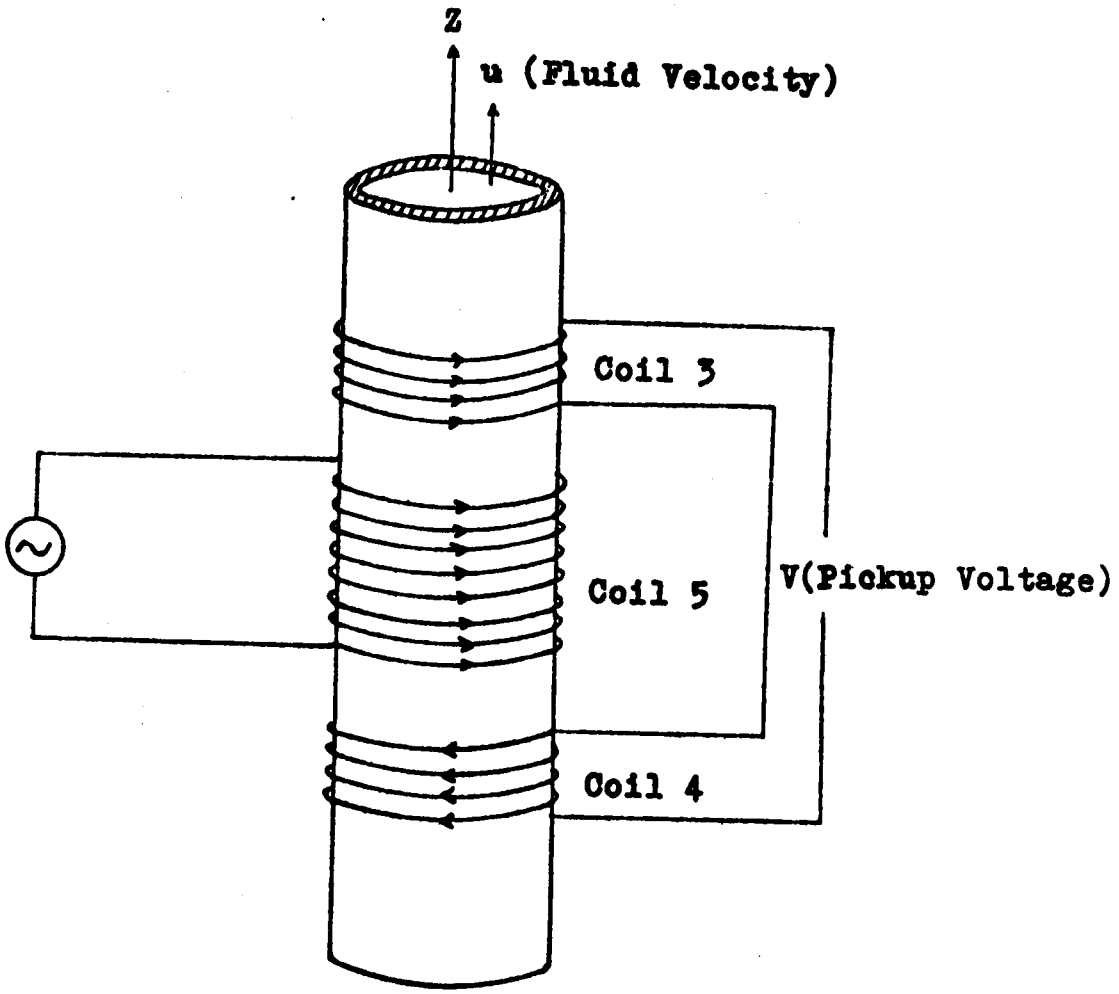


Figure 4. Directions and connections of winding of the three-coil system.

$$M_{45} = i\omega\left(\frac{n'}{N}\right)\left(\frac{n}{N}\right)h\mu_o \sum_{\text{coil } 4} 2\pi(m-1)A_{n,m} , \tag{4.2}$$

If the driving current in the driver coil is I, the induced voltages at coil 3 and coil 4 are

$$V_3 = iI\omega\left(\frac{n'}{N}\right)\left(\frac{n}{N}\right)h\mu_o \sum_{\text{coil } 3} 2\pi(m-1)A_{n,m} , \tag{4.3}$$

$$V_4 = iI\omega\left(\frac{n'}{N}\right)\left(\frac{n}{N}\right)h\mu_o \sum_{\text{coil } 4} 2\pi(m-1)A_{n,m} , \tag{4.4}$$

respectively. Since the pickup coils are opposite in direction, the total induced voltage would be

$$V = V_3 - V_4$$

$$= iI\omega\left(\frac{n'}{N}\right)\left(\frac{n}{N}\right)h\mu_o \left\{ \sum_{\text{coil } 3} 2\pi(m-1)A_{n,m} - \sum_{\text{coil } 4} 2\pi(m-1)A_{n,m} \right\}, \tag{4.5}$$

If the velocity of the liquid metal is zero, the contours of equal vector potential are symmetric with respect to coil 5. Therefore

$$\sum_{\text{coil } 3} 2\pi(m-1)A_{n,m} = \sum_{\text{coil } 4} 2\pi(m-1)A_{n,m} , \tag{4.6}$$

and

$$V = 0 .$$

If the velocity of the liquid metal is not zero, the vector potential will be slightly displaced in the direction of the velocity, so that

$$\sum_{\text{coil } 3} 2\pi(m-1)A_{n,m} \neq \sum_{\text{coil } 4} 2\pi(m-1)A_{n,m} . \tag{4.7}$$

If I, n, N, n´, N´,ω, and velocity are kept constant, then

$$V \propto \left[\sum_{\text{coil } 3} 2\pi(m-1)A_{n,m} - \sum_{\text{coil } 4} 2\pi(m-1)A_{n,m} \right] . \qquad (4.8)$$

Five-Coil System

In order to maximize the total induced voltage, we have to maximize the difference of the vector potential between the two separated pickup coils, to have the biggest velocity effect on the vector potential. Let us consider the velocity term $\mu\sigma u\frac{\partial A}{\partial z}$, where $\frac{\partial A}{\partial z}$ is the rate of change of the vector potential along the z-direction. If we increase $\frac{\partial A}{\partial z}$, the velocity term would also be increased. Therefore we introduce the five-coil system. In this system, we have three driver coils and two pickup coils as shown in Figure 5. Coil 2 and coil 6 are the two end driver coils. They are identical to each other and symmetrically situated with respect to the central driver coil, but their directions of winding are opposite to that of the central driver coil. All three driver coils are connected in series as shown in Figure 6.

These two end driver coils give a more rapid rate of change of the vector potential with respect to the axial coordinate z, as shown in Figures 7 and 8. The cross-sections of the systems and the contours of equal vector potential are shown in the top part of the figures. In the lower part of the two figures are shown the vector potential

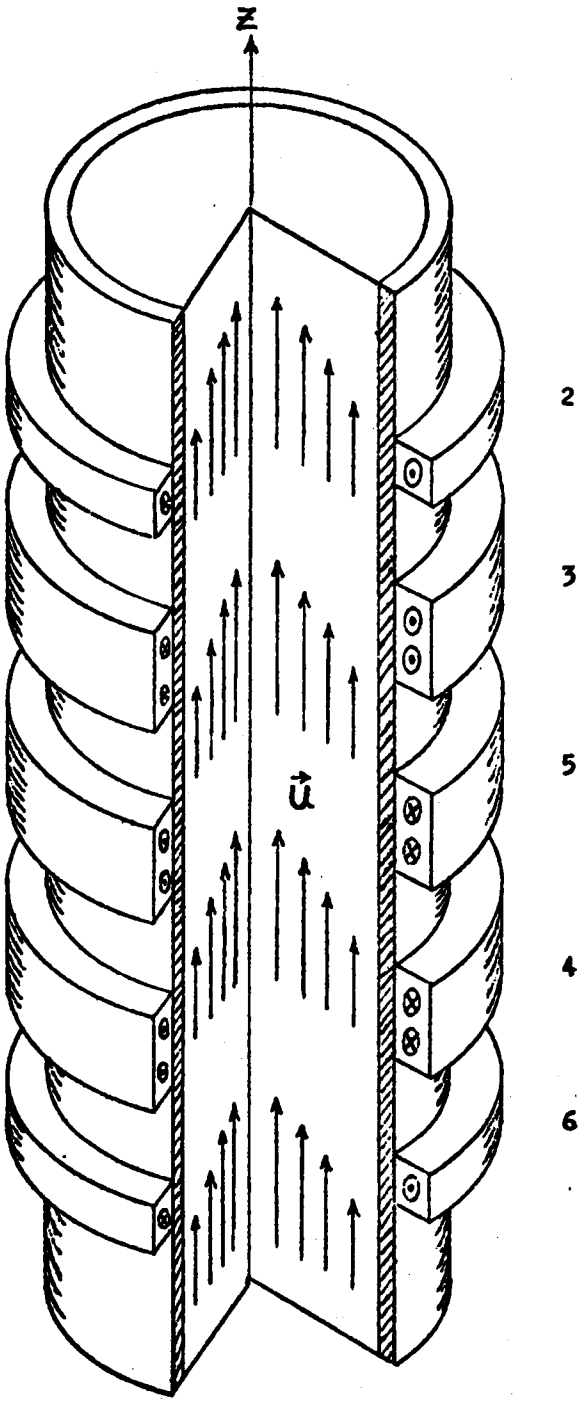


Figure 5. Diagram of five-coil flowmeter arrangement.

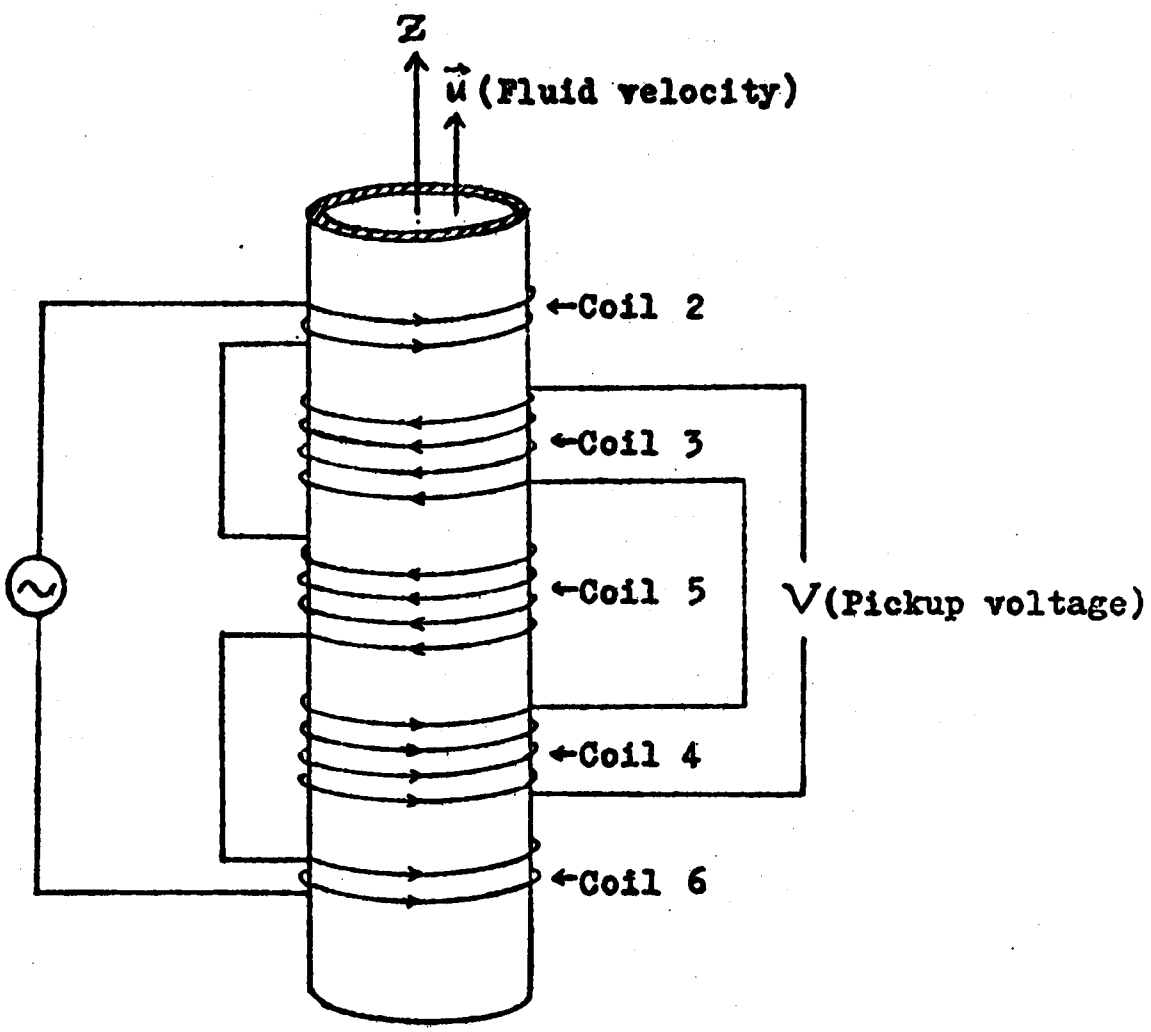


Figure 6. Directions and connections of winding of the five-coil system.

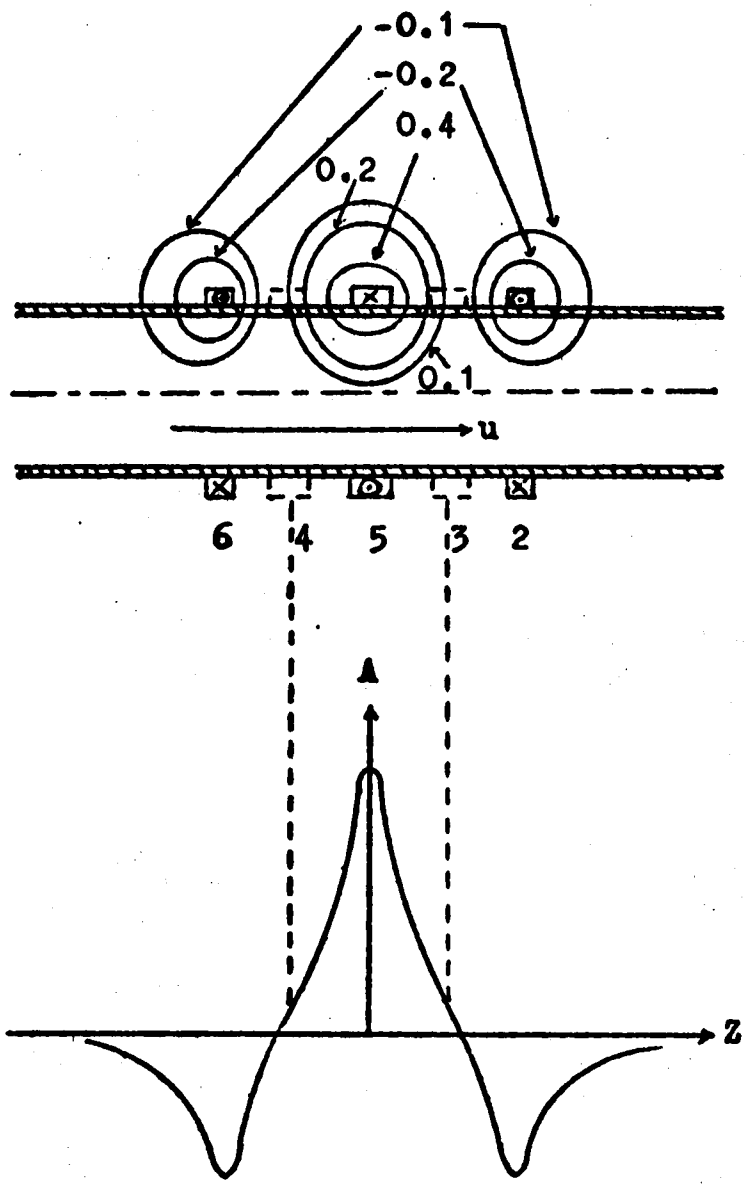


Figure 7. Five-coil system, triple driver.

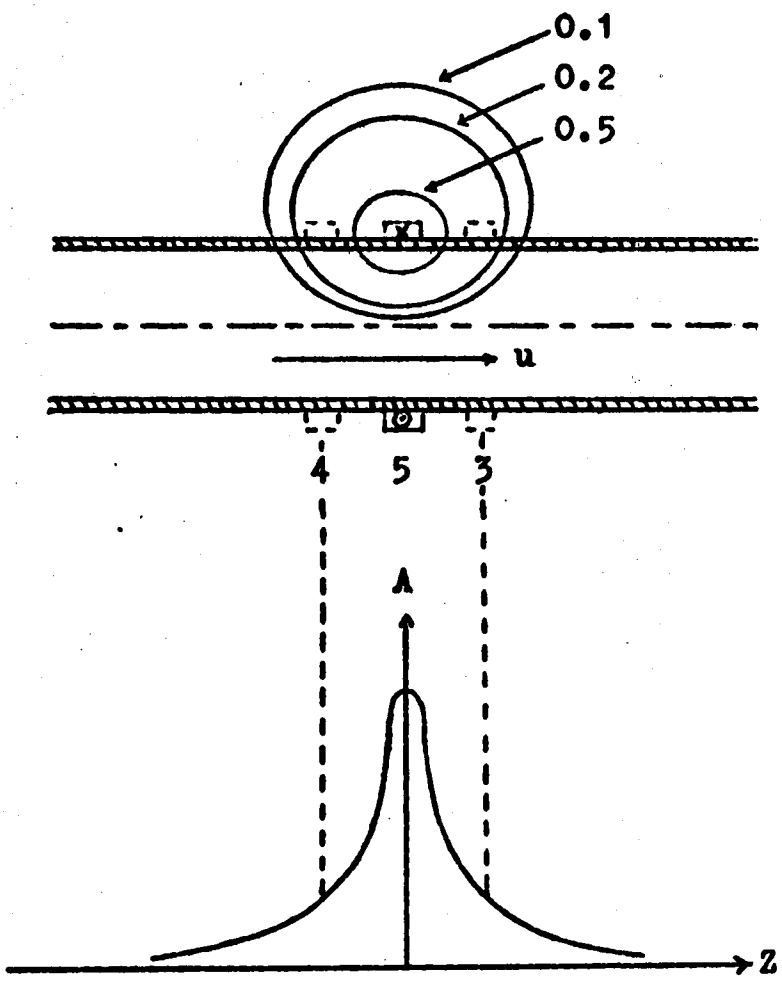


Figure 8. Three-coil system, single driver.

produced by the driver coils at the radius of the first layer of coils. Comparing these two figures, we see that, at the positions where the pickup coils are located, the value of $\left|\frac{\partial A}{\partial z}\right|$ for the five-coil system is much greater than that for the three-coil system.

The distance between the central driver coil and the end driver coil is also an important factor. If the end driver coils are too close to the central driver coil, the vector potentials generated by the central driver coil and the two end driver coils would nearly cancel each other. Thus the total induced voltage at the pickup coils would become even smaller. If these two end driver coils are too far away from the central driver coil, there will be no increase in the rate of change of the vector potential along the z-direction. Therefore we have to find the optimum distance that will produce the maximum induced voltage in the pickup coils.

Let n" be the no. of turns of wire in driver coil 2,

N" be the no. of lattice points in driver coil 2,

n be the no. of turns of wire in driver coil 5,

N be the no. of lattice points in driver coil 5,

n"' be the no. of turns of wire in driver coil 6,

N"' be the no. of lattice points in driver coil 6,

n' be the no. of turns of wire in pickup coil 3 or 4,

N' be the no. of lattice points in pickup coil 3 or 4

We use wire of the same size in the driver coils,

$$\therefore \frac{n}{N} = \frac{n''}{N''} = \frac{n'''}{N'''} \quad . \tag{4.9}$$

By equation (3.27), the mutual impedance between coil 3 and coil 2, coil 3 and coil 5, coil 3 and coil 6 are given by

$$M_{32} = i\omega \left(\frac{n'}{N'}\right) \left(\frac{n''}{N''}\right) h\mu_o \sum_{\text{coil } 3} 2\pi (m-1) A^{(2)}_{n,m}$$

$$= i\omega \left(\frac{n'}{N'}\right) \left(\frac{n}{N}\right) h\mu_o \sum_{\text{coil } 3} 2\pi (m-1) A^{(2)}_{n,m} \quad , \tag{4.10}$$

$$M_{35} = i\omega \left(\frac{n'}{N'}\right) \left(\frac{n}{N}\right) h\mu_o \sum_{\text{coil } 3} 2\pi (m-1) A^{(5)}_{n,m} \quad , \tag{4.11}$$

$$M_{36} = i\omega \left(\frac{n'}{N'}\right) \left(\frac{n'''}{N'''}\right) h\mu_o \sum_{\text{coil } 3} 2\pi (m-1) A^{(6)}_{n,m}$$

$$= i\omega \left(\frac{n'}{N'}\right) \left(\frac{n}{N}\right) h\mu_o \sum_{\text{coil } 3} 2\pi (m-1) A^{(6)}_{n,m} \quad , \tag{4.12}$$

where $A^{(2)}_{n,m}$, $A^{(5)}_{n,m}$, and $A^{(6)}_{n,m}$ are the vector potentials at lattice point (n,m) generated by driver coils 2, 5 and 6, respectively.

Therefore the mutual impedance between the pickup coil 3 and the driver coils is given by

$$M_3 = M_{35} - M_{32} - M_{36}$$

$$= i\omega \left(\frac{n'}{N'}\right) \left(\frac{n}{N}\right) h\mu_o \sum_{\text{coil } 3} 2\pi (m-1) \left(A^{(5)}_{n,m} - A^{(2)}_{n,m} - A^{(6)}_{n,m}\right) \quad . \tag{4.13}$$

Similarly the mutual impedance between the pickup coil 4 and

the driver coils is given by

$$M_4 = M_{45} - M_{42} - M_{46}$$

$$= i\omega\left(\frac{n'}{N}\right)\left(\frac{n}{N}\right)h\mu_o \sum_{\text{coil } 4} 2\pi(m-1)\left(A^{(5)}_{n,m} - A^{(2)}_{n,m} - A^{(6)}_{n,m}\right) . \qquad (4.14)$$

The induced voltages at pickup coil 3 and pickup coil 4 are given by

$$V_3 = IM_3 = iI\omega\left(\frac{n'}{N}\right)\left(\frac{n}{N}\right)h\mu_o \sum_{\text{coil } 3} 2\pi(m-1)\left(A^{(5)}_{n,m} - A^{(2)}_{n,m} - A^{(6)}_{n,m}\right) ,$$

$$V_4 = IM_4 = iI\omega\left(\frac{n'}{N}\right)\left(\frac{n}{N}\right)h\mu_o \sum_{\text{coil } 4} 2\pi(m-1)\left(A^{(5)}_{n,m} - A^{(2)}_{n,m} - A^{(6)}_{n,m}\right) . \qquad (4.15)$$

Since the pickup coils 3 and 4 are wound in opposition, thus the total pickup voltage will be

$$V = V_3 - V_4$$

$$= iI\omega\left(\frac{n'}{N}\right)\left(\frac{n}{N}\right)h\mu_o \left[\sum_{\text{coil } 3} 2\pi(m-1)\left(A^{(5)}_{n,m} - A^{(2)}_{n,m} - A^{(6)}_{n,m}\right)\right.$$

$$\left. - \sum_{\text{coil } 4} 2\pi(m-1)\left(A^{(5)}_{n,m} - A^{(2)}_{n,m} - A^{(6)}_{n,m}\right)\right]$$

$$= iI\omega\left(\frac{n'}{N}\right)\left(\frac{n}{N}\right)h\mu_o (SA) , \qquad (4.16)$$

where $SA = \left[\sum_{\text{coil } 3} 2\pi(m-1)\left(A^{(5)}_{n,m} - A^{(2)}_{n,m} - A^{(6)}_{n,m}\right)\right.$

$$\left. - \sum_{\text{coil } 4} 2\pi(m-1)\left(A^{(5)}_{n,m} - A^{(2)}_{n,m} - A^{(6)}_{n,m}\right)\right] . \qquad (4.17)$$

Optimum Distance and Optimum Position

We shall find the optimum distance which will give the maximum value of SA. We divide the quarter-plane into 120 × 54 lattice points as shown in Figure 9. The distance between lattice points is h = 0.014"; the inside radius of the tube is R_1 = 7.5h; the outside radius of the tube is R_2 = 8.5h. We shall assume the liquid metal to be mercury, and the velocity of the mercury to be 20cm/sec. The axial length of the central driver coil, the end driver coils and the pickup coils are assumed to be 4h, 2h and 1h respectively, and the thickness of all coils are assumed to be single layer of lattice points. Using equations (3.19), (3.11), and (4.17), the value of SA can be calculated by computer for various positions of the pickup coils and for various spacing (from 1h to 16h) between the central driver and the end driver coils.

The calculated results for the frequencies of 1 KHz, 10 KHz and 20 KHz are plotted in Figure 10 as the distance curve. The ordinate represents the value of SA, while the abscissa stands for the distance between the central driver and the end driver coils in units of h. In the same manner, we can calculate the corresponding results for double layer and triple layer of lattice points. The results are shown in Figure 10, from which we see that the optimum spacing between driver coils should be about 11h for single layer coil and 12h for double layer and triple layer coils.

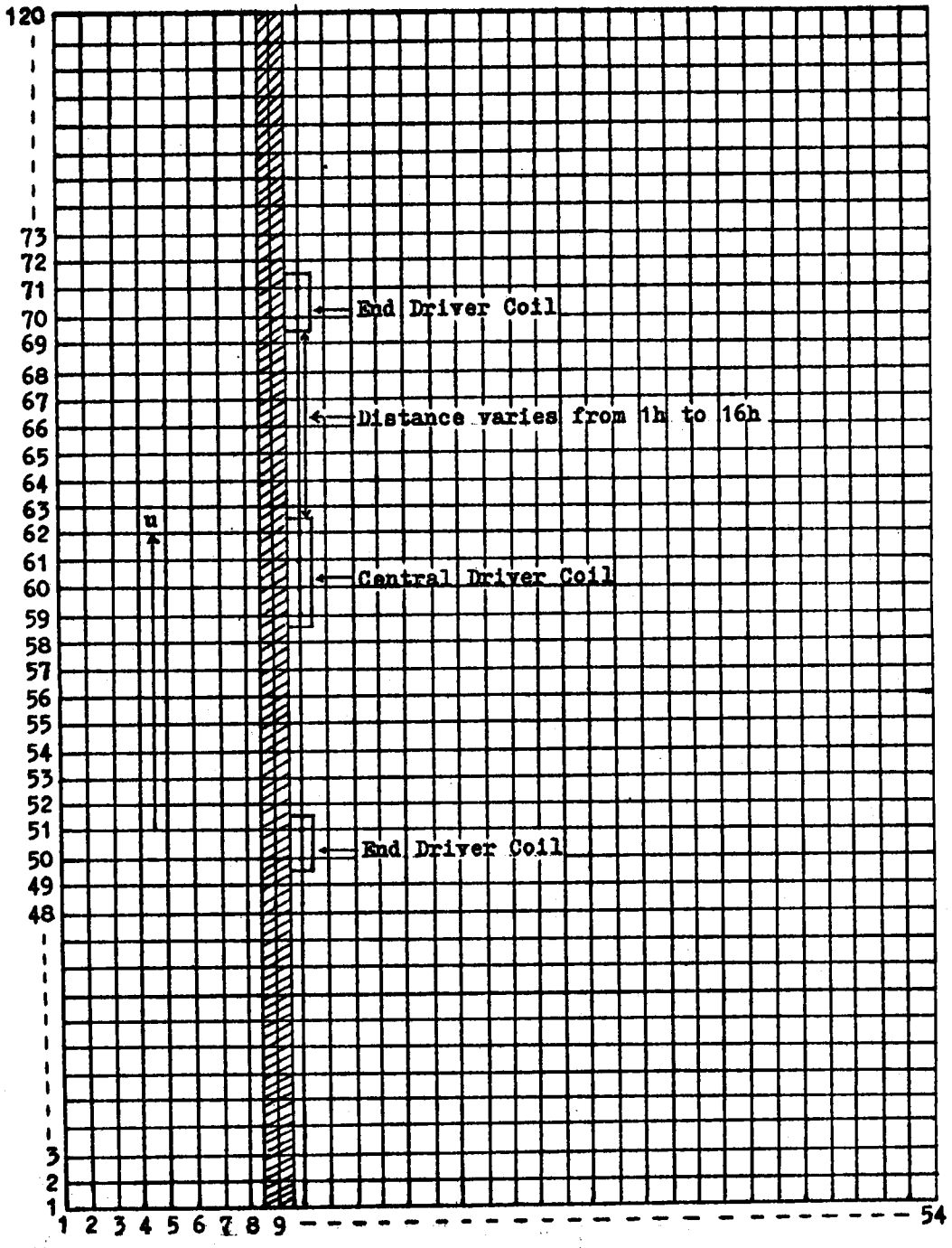


Figure 9. Layout of the single layer, five-coil system on a lattice points.

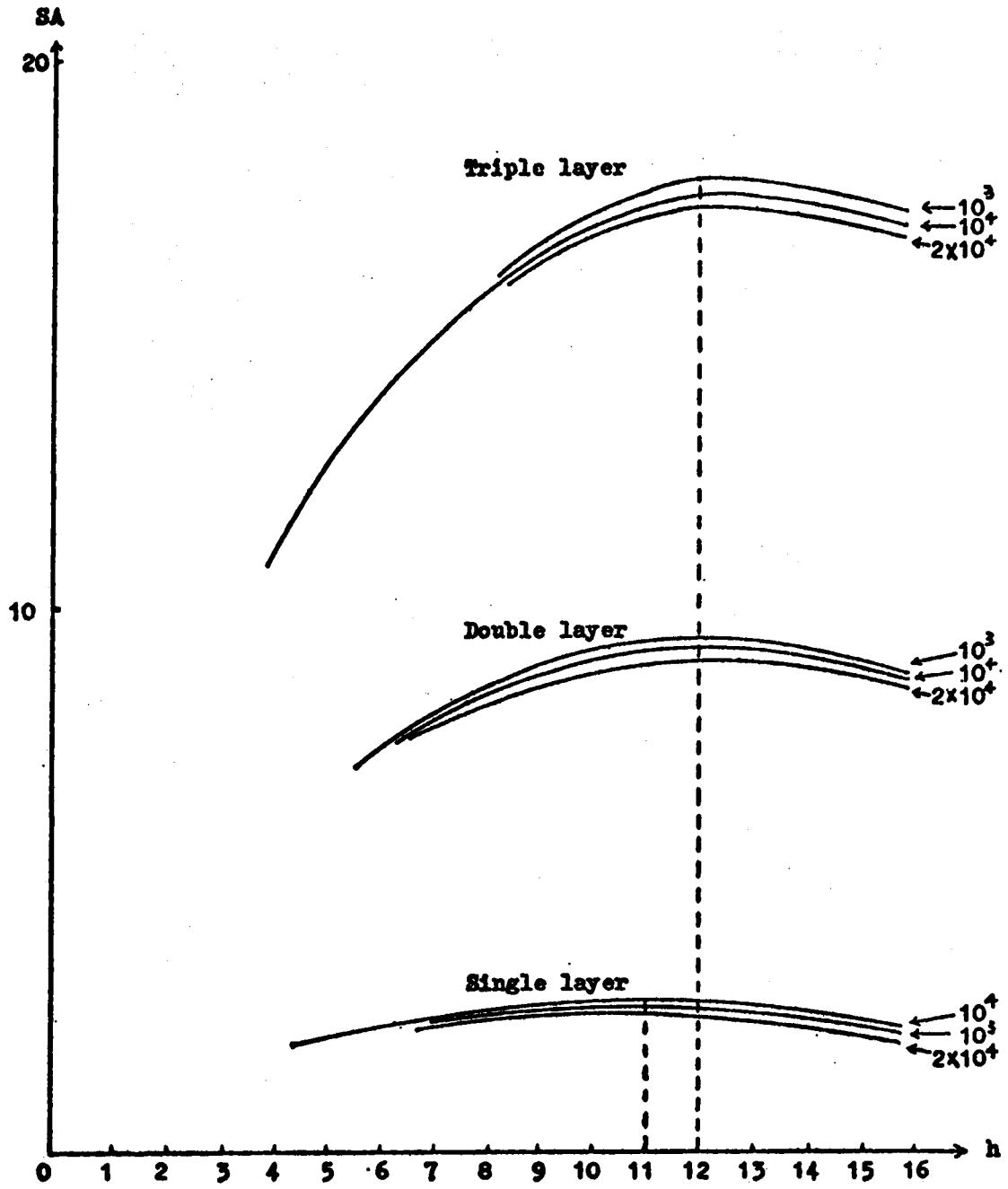


Figure 10. Optimum driver coil separation.

For the optimum distance, we can construct the position curves in Figure 11. The curves show that locating the pickup coil at a lattice spacing of 5h from the central driver coil for single layer and 6h for double and triple layer, give the maximum value of SA. We also show the corresponding position curve for a single layer three-coil system in Figure 11. Comparing with the position curve of five-coil system shows that the five-coil system yields a greater pickup voltage for the given conditions.

It also appears that the three-layer system will give the greatest voltage. This would be true if the driving current were really constant. However, in a practical circuit, the amplifier which supplies the driver current is usually voltage-limited (for producing a sinusodial current) so that the greater resistance of the three-layer coil reduces the available driving current and may cause the output voltage of the pickups to be less than that for the double layer coil. Therefore we have to analyze the circuit of the five-coil system for the various numbers of layers to find the optimum (1) frequencies, (2) number of layers of lattice points, and (3) size of the wire.

The equivalent circuit for the five-coil system is shown in Figure 12. We can write the equations for the drops in voltage around each of the loops in the circuit, in terms of the parameters listed below:

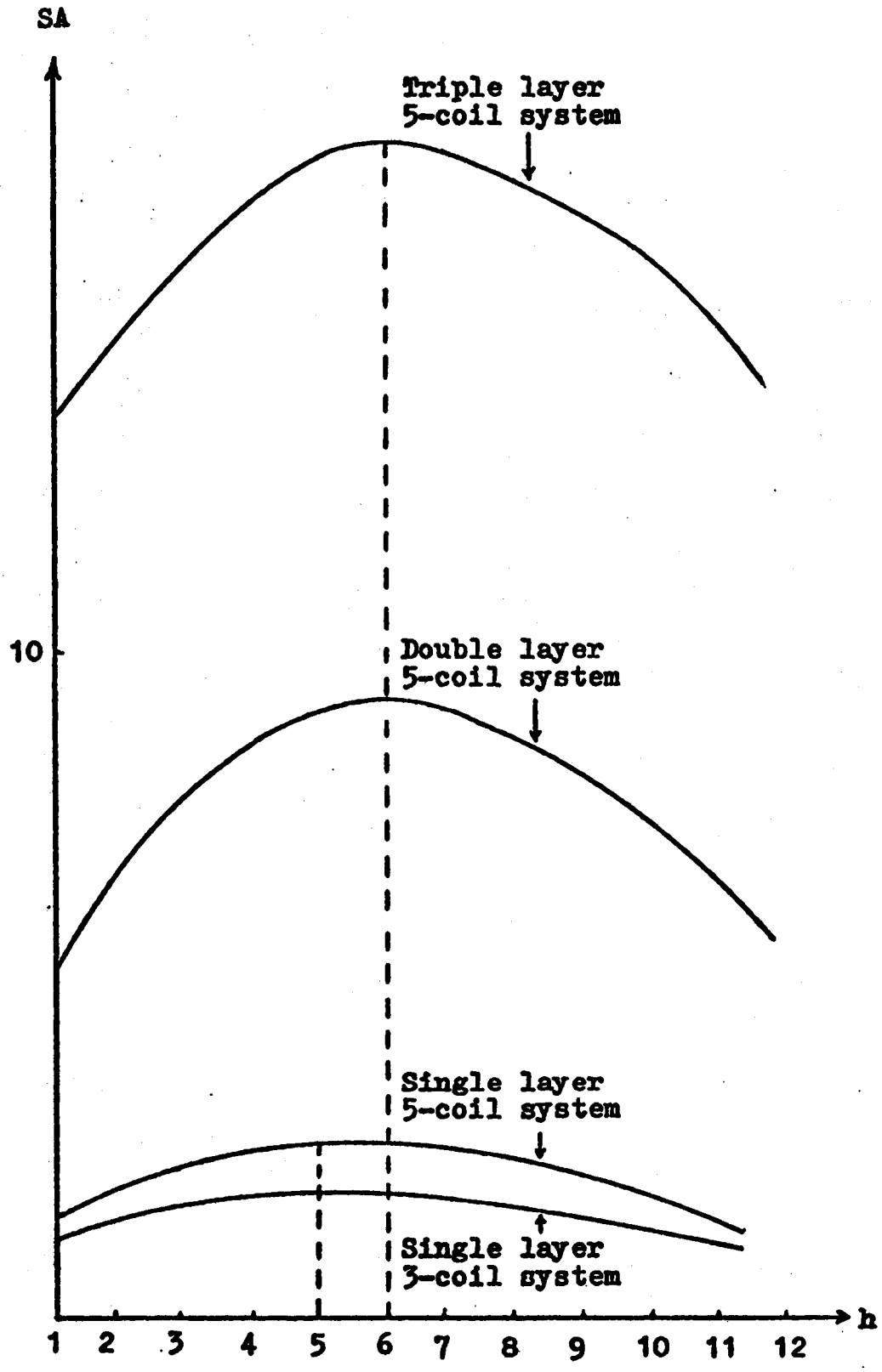


Figure 11. Optimum pickup coil position.

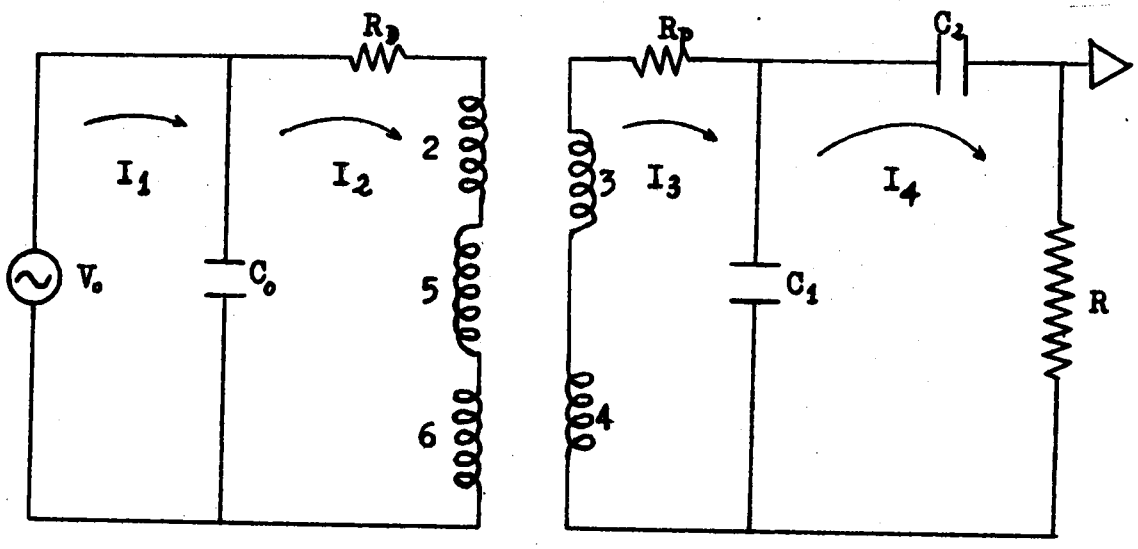


Figure 12. Equivalent circuit for the five-coil system.

V_o , Driving voltage

I , Loop current

R_D , D.C. resistance of driver coil

R_P , D.C. resistance of pickup coil

C_o , Shunt capacitance of driver coil

C_1 , Shunt capacitance of pickup coil

C_2 , Series capacitance of pickup coil

M_{34}, Mutual inductance between coil 3 and coil 4

M_{25}, Mutual inductance between coil 2 and coil 5

M_{26}, Mutual inductance between coil 2 and coil 6

M_{56}, Mutual inductance between coil 5 and coil 6

M_1 , Mutual inductance between driver coils and pickup coil 3

M_2 , Mutual inductance between driver coils and pickup coil 4

L_2 , Self inductance of coil 2

L_3 , Self inductance of coil 3

L_4 , Self inductance of coil 4

L_5 , Self inductance of coil 5

L_6 , Self inductance of coil 6

Then the impedance of the pickup coils can be expressed as

$$Z_P = i\omega(L_3+L_4-2M_{34}) \ , \qquad (4.18)$$

and the impedance of the driver coils can be expressed as

$$Z_D = i\omega(L_2 +L_5 +L_6 -2M_{25} -2M_{56} +2M_{26}). \qquad (4.19)$$

Kirchhoff's law applied to the various circuits yields the following equations

$$I_1(-\frac{i}{\omega C_o}) - I_2(-\frac{i}{\omega C_o}) = V_o \ , \tag{4.20}$$

$$-I_1(-\frac{i}{\omega C_o}) + I_2(Z_D+R_D-\frac{i}{\omega C_o}) - I_3(i\omega M_1-i\omega M_2) = 0 \ , \tag{4.21}$$

$$I_2(i\omega M_1-i\omega M_2) + I_3(Z_p+R_p-\frac{i}{\omega C_1}) - I_4(-\frac{i}{\omega C_1}) = 0, \tag{4.22}$$

$$-I_3(-\frac{i}{\omega C_1}) + I_4(R-\frac{i}{\omega C_1}-\frac{i}{\omega C_2}) = 0. \tag{4.23}$$

Solving for the loop currents by computer and substituting I_2 into equation (4.16), we find that the total induced voltage at the pickup coils is given by

$$V = i\omega I_2(\frac{n}{N})(\frac{n}{N})h\mu_o(SA) \ . \tag{4.24}$$

We have calculated the total induced voltage for single layer, double layer and triple layer coils at the optimum distances by computer. From Figure 11, we know that the optimum position for the pickup coils is at the point 6h for double and triple layer, and 5h for single layer, but points at 5h, 7h and 8h for double and triple layer, and 4h, 6h, 7h for single layer also give quite large values of SA. Therefore the pickup coil is chosen to be 4h long and located at sites 4h-7h for single layer, and sites 5h-8h for the double and triple layer coils. The configurations are shown in

Figure 13. We assume the following values for the parameters:

V_o = 10 volts, peak to peak,

$C_o = 1.3 \times 10^{-10}$ farad,

$C_1 = 1.5 \times 10^{-10}$ farad,

$C_2 = 2.2 \times 10^{-9}$ farad.

R_D and R_P are determined by the number of layers and the gauge number of wire. The mutual inductances and self inductances can be calculated by using equations (3.27) and (3.28). Then the pickup voltages for various frequencies and various gauge numbers of wire at a given velocity can be calculated. The results show that the gauge number of wire does not affect the pickup voltage much, thus we only plot the pickup voltage as a function of operating frequency in Figure 14. It is evident that the double layer coil gives the greatest pickup voltage. Therefore we come to the conclusion that we should use a double layer five-coil system, and the system can operate well at frequencies from 5KHz to 100KHz for the dimensions and liquid metal (mercury) chosen. The configuration is shown in Figure 15.

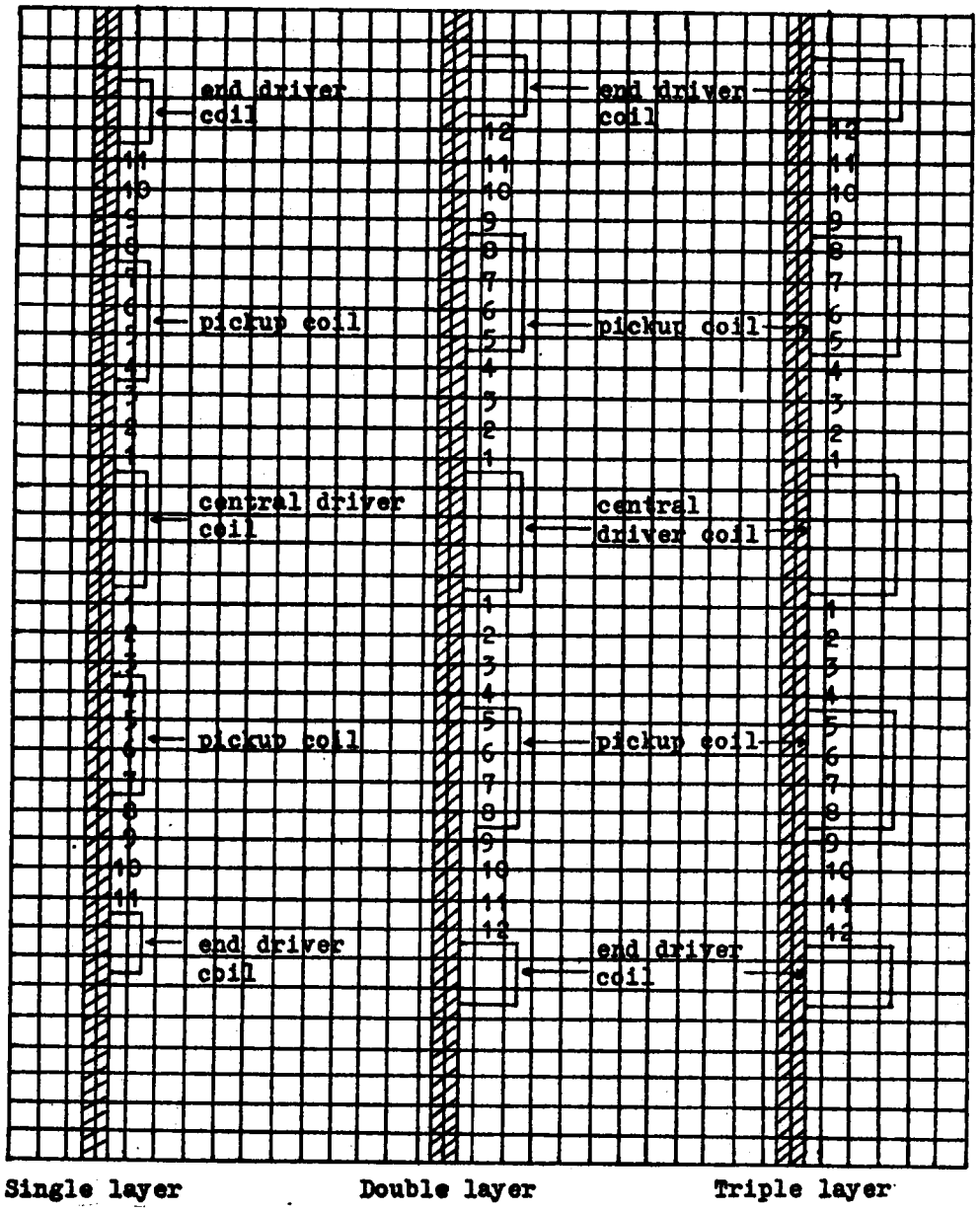


Figure 13. Configuration of single layer, double layer and triple layer coils.

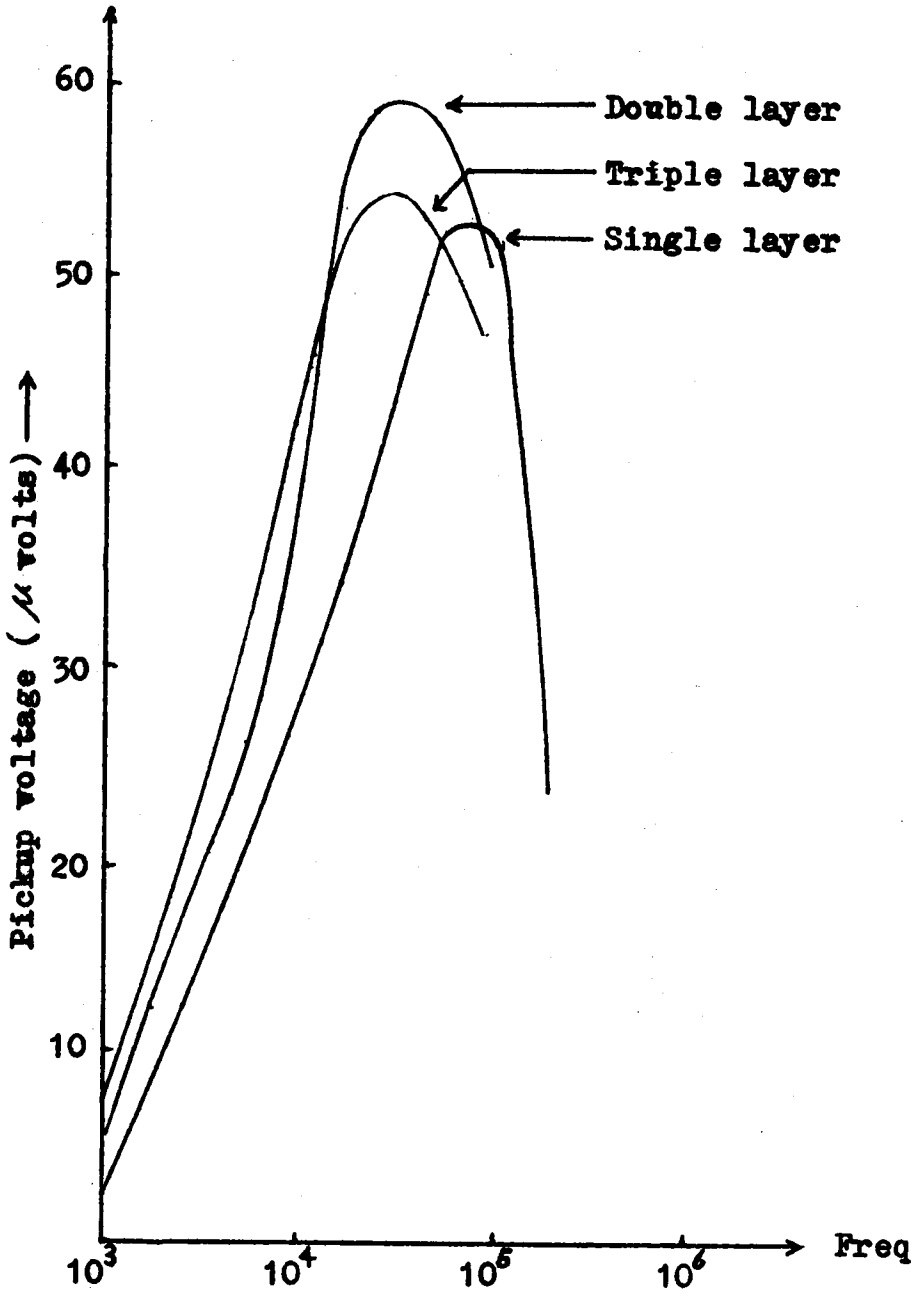


Figure 14. Pickup voltage as a function of operating frequency.

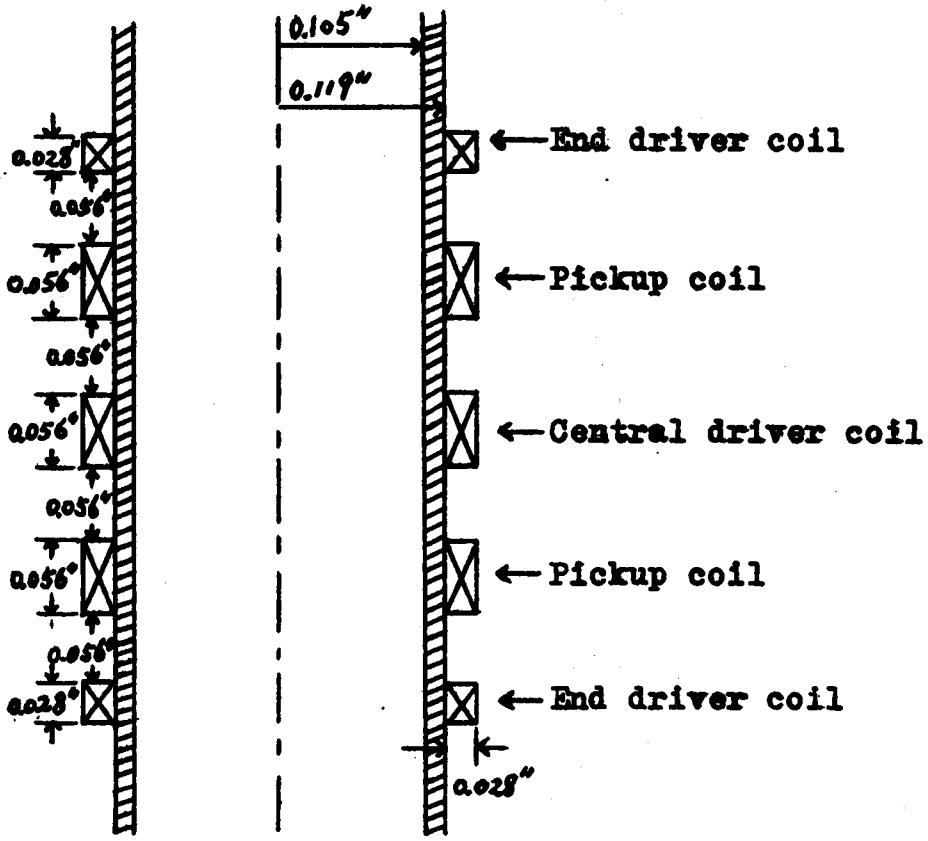


Figure 15. Diagram of double layer five-coil system.

CHAPTER 5

EXPERIMENT

One five-coil system probe tube and one three-coil system probe tube were constructed. Calculations and measurements have been made on both tubes.

Five-Coil System Probe Tube

The dimension of the five-coil system probe tube is the same as shown in Figure 15. The central driver coil is wound with 288 turns of no. 44 copper wire, each end driver coil is wound with 144 turns of no. 44 copper wire and each pickup coil is wound with 800 turns of no. 48 copper wire. The driving voltage V_o = 10 volts peak to peak, the D.C. resistance of the driver coils R_D = 107.75 ohms, and the D.C. resistance of the pickup coils R_p = 799.20 ohms. The arrangement of the experimental apparatus is shown in Figure 16. The apparatus consists of two mercury containers, one variable speed pump and the probe tube. We chose mercury as the liquid metal. The pickup voltages were measured at various mercury average velocities at the frequencies of 5KHz, 10KHz, 20KHz, 50KHz and 100KHz.

The calculations were repeated for several assumed velocity profiles. One type of distribution used in the

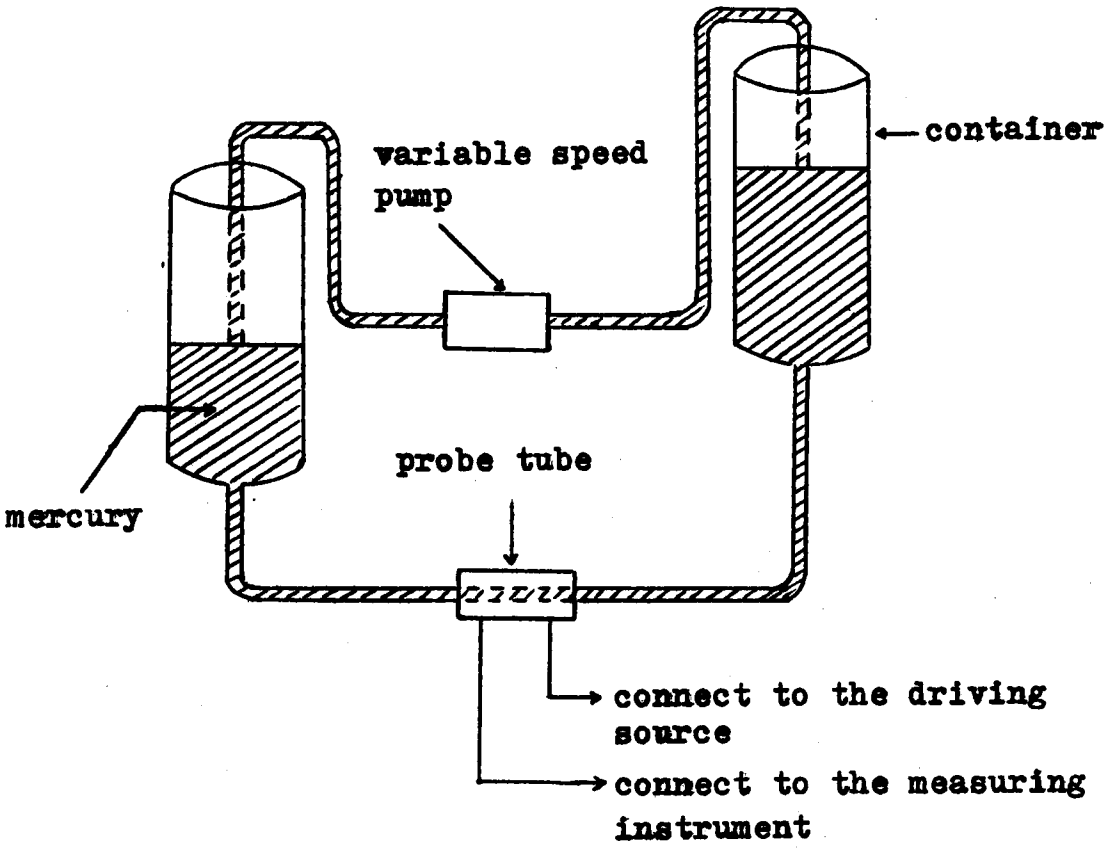


Figure 16. Diagram of the experimental apparatus.

calculations was

$$u(r) = u_{av}\left[1 - \left(\frac{r}{a}\right)^{k}\right] , \qquad (5.1)$$

where a is the radius of the tube and u_{av} is the average velocity which would give the same total flow rate if the velocity were constant everywhere inside the tube, corresponding to $k = \infty$. The parabolic profile ($k = 2$) should occur for laminar viscous flow. For the conditions of the experiment, it was expected that the flow would be turbulent. Among the various turbulent flow profiles we have used are the Prandtl power law (14)

$$u(r) = \frac{60}{49}\, u_{av}\left[1-\left(\frac{r}{a}\right)\right]^{\frac{1}{7}}, \qquad (5.2)$$

and the theoretical velocity distribution of Pai (15),

$$u(r) = 1.1748u_{av}\left[1-0.204\left(\frac{r}{a}\right)^{2} - 0.796\ \left(\frac{r}{a}\right)^{32}\right] . \qquad (5.3)$$

These velocity distributions are plotted in Figure 17, along with three ad hoc profiles, marked v_1, v_2, and v_3, which represent flow patterns intermediate between laminar and turbulent flow.

The results of the measured values and the calculated values for constant velocity profile ($k = \infty$) are shown in Figures 18, 19, 20, 21 and 22. At high frequencies, the penetration depth of the eddy-currents was so small that only the velocities near the wall of the tube were measured,

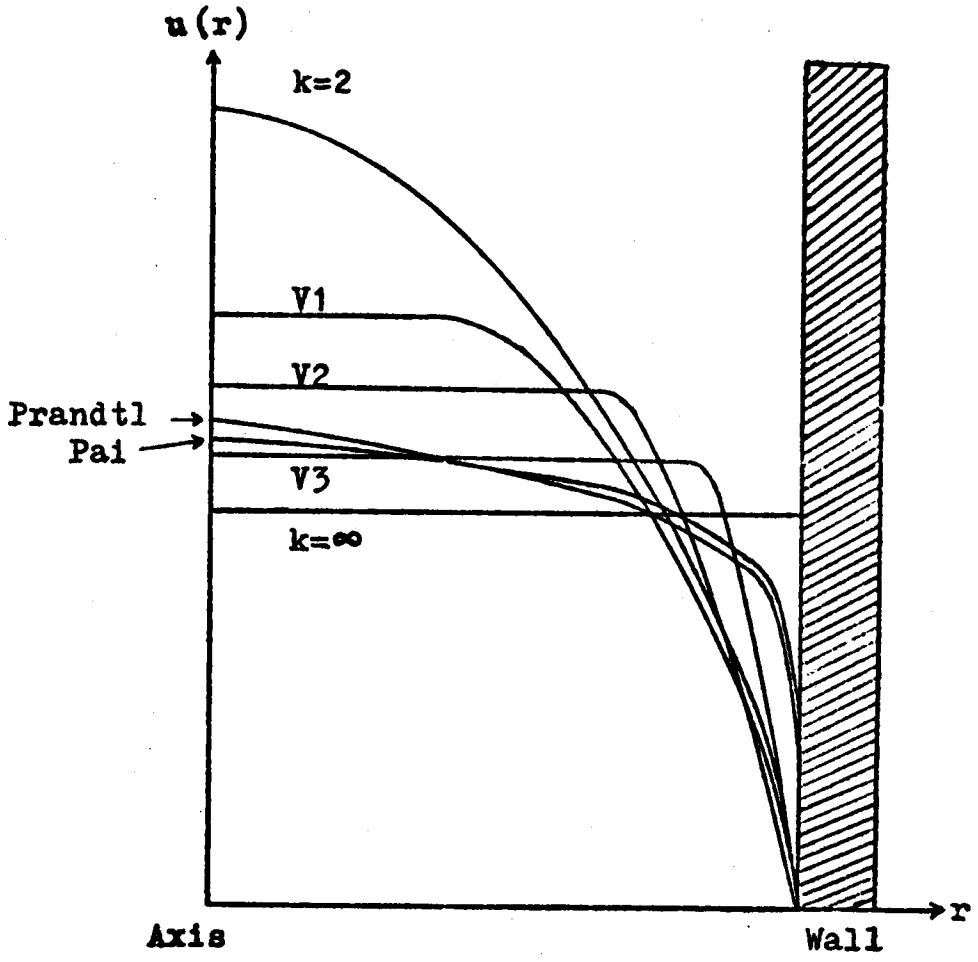


Figure 17. Some possible velocity distributions.

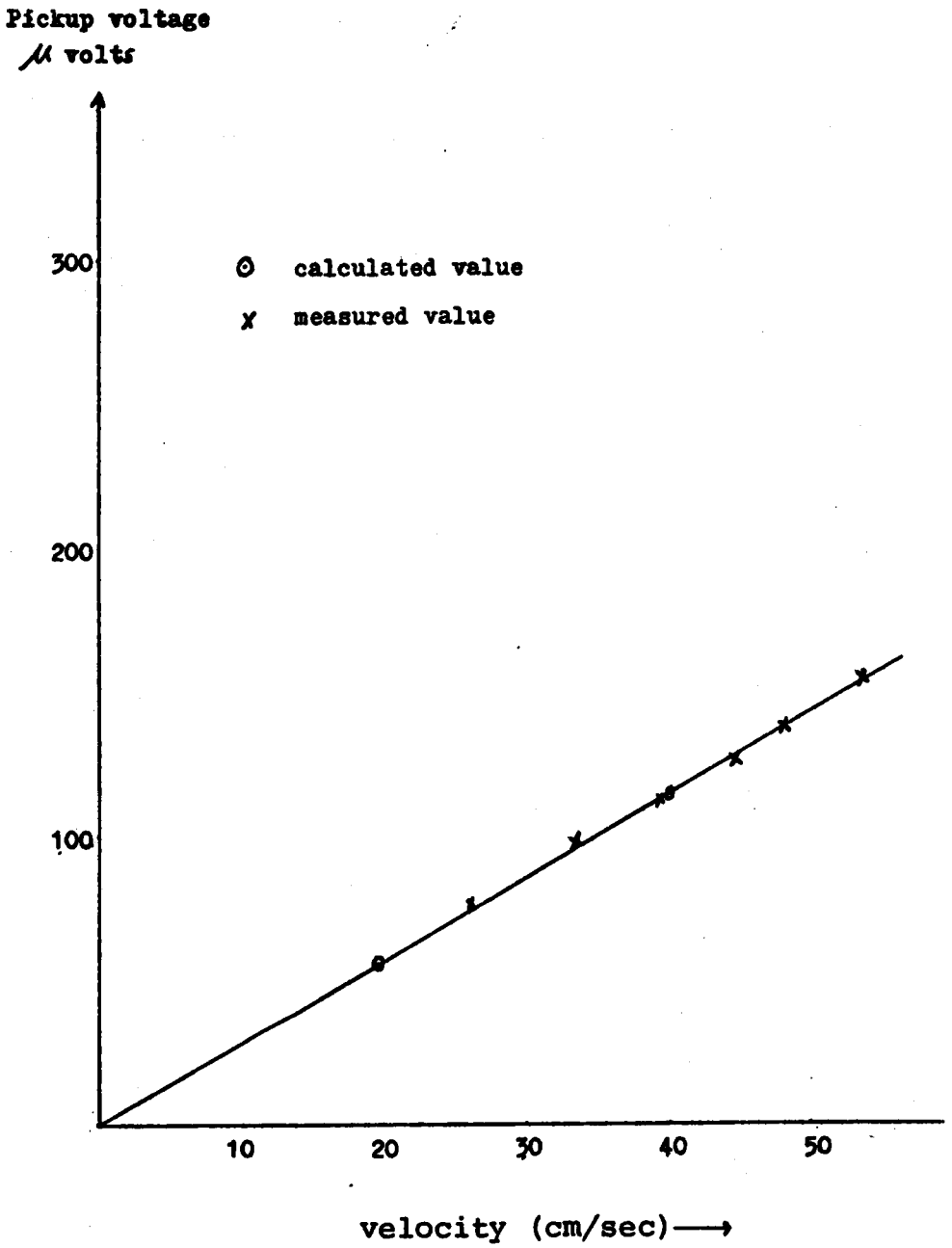


Figure 18. Measured values and calculated values at the frequency of 5 x 10^3 cycles per second.

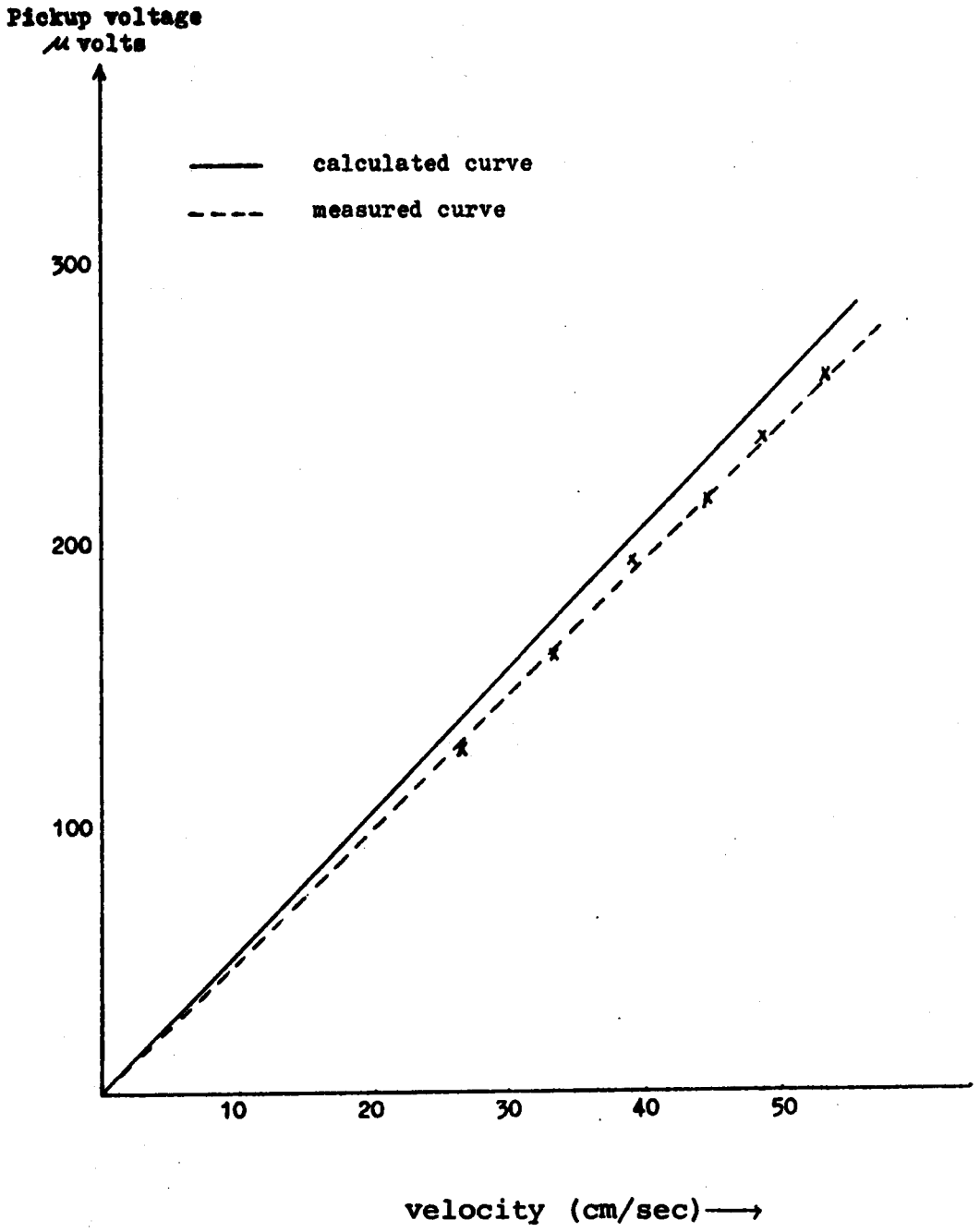


Figure 19. Measured values and calculated values at the frequency of 10^4 cycles per second.

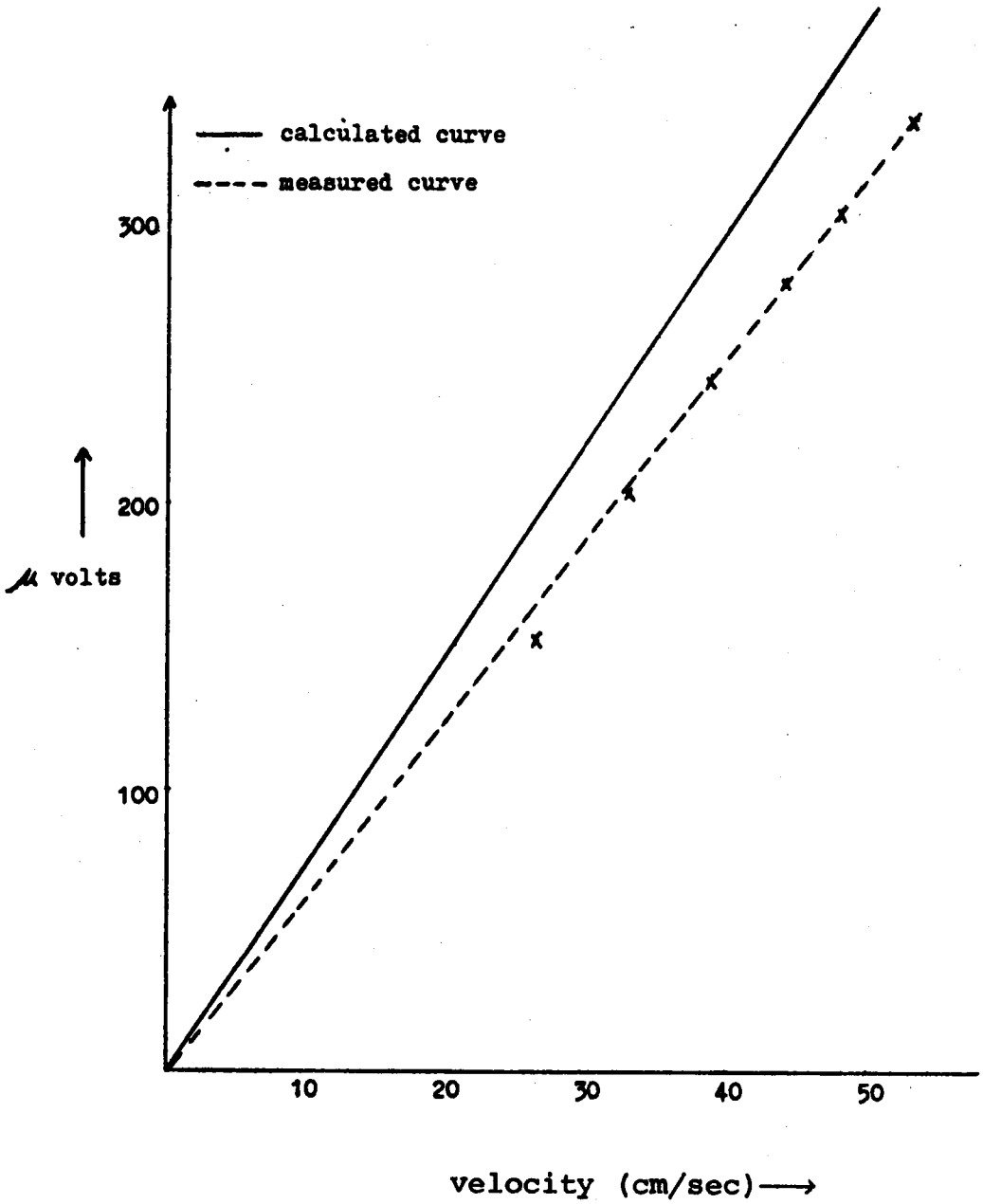


Figure 20. Measured values and calculated values at the frequency of 2×10^4 cycles per second.

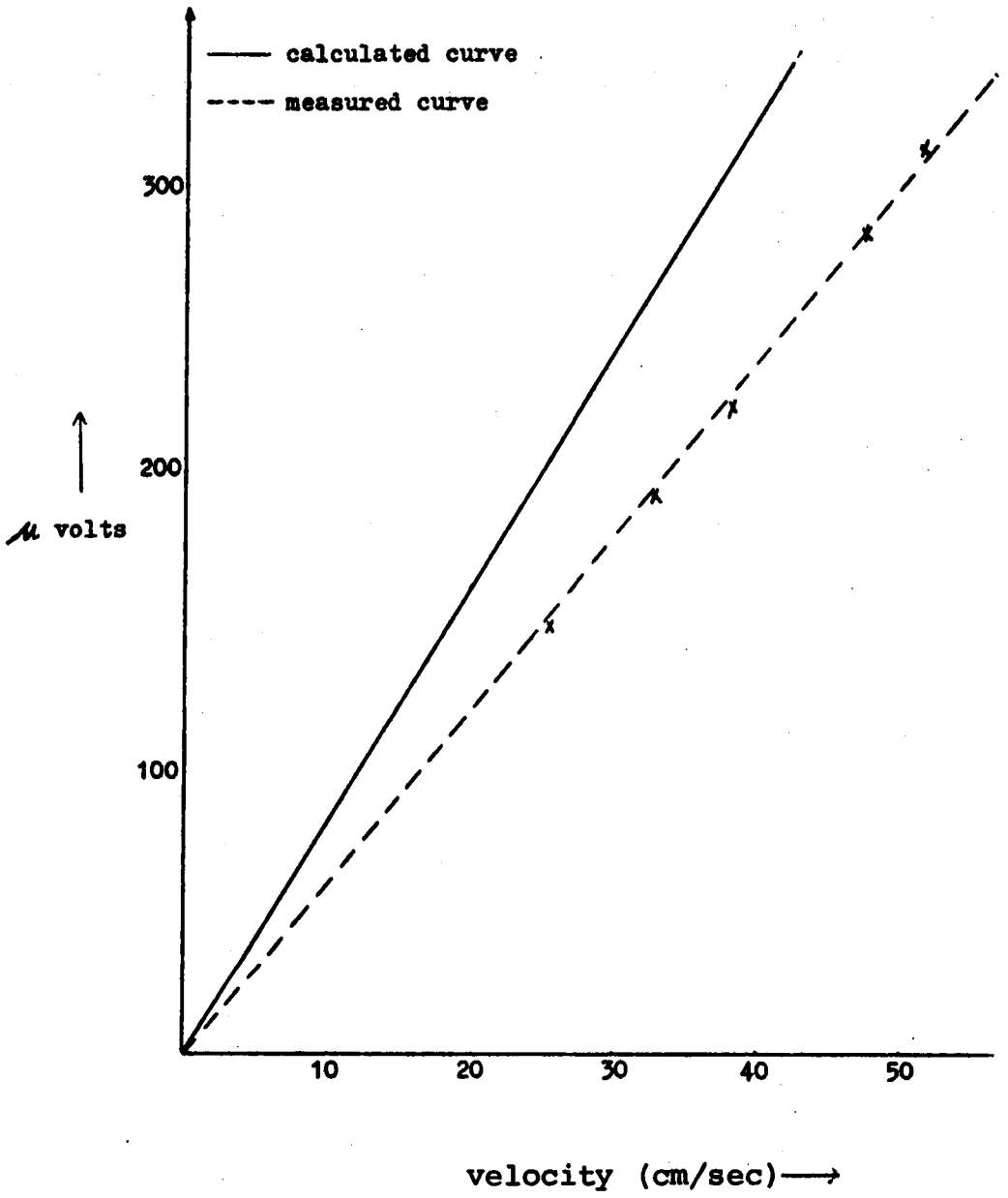


Figure 21. Measured values and calculated values at the frequency of 5×10^4 cycles per second.

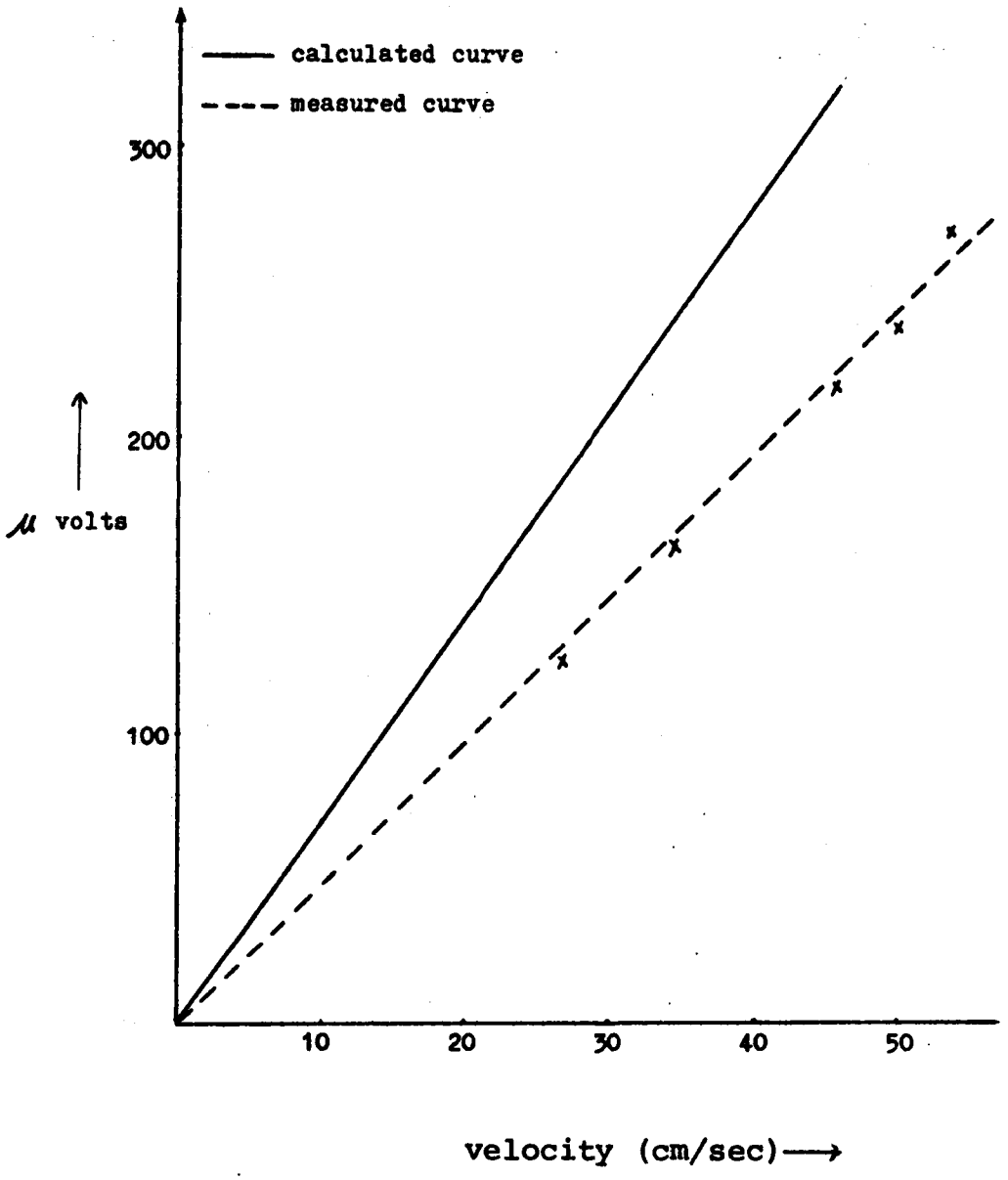


Figure 22. Measured values and calculated values at the frequency of 10^5 cycles per second.

and these are much less than the average velocity. This effect is shown in Figures 21 and 22, where the experimental voltages fall far below the theoretical ones. However at low frequencies the eddy-currents were penetrating deeply into the fluid, thus the experimental and the theoretical values are in excellent agreement, as shown in Figures 18, 19 and 20.

In an attempt to fit the experimental data at all frequencies and to evaluate the flow velocity profiles, we have calculated the slope of the voltage vs average velocity curve for various frequencies and various assumed velocity profiles. The results are shown in Figure 23, where the solid curves represent the theoretical slopes for the velocity profiles given in Equations (5.1), (5.2), and (5.3). At the low frequency of 5 KHz the experimental results agree with the constant velocity profile ($k = \infty$) or the turbulent flow profiles. At very high frequencies, the experimental measurements are very difficult so that the accuracy is limited, but the experimental voltages and slopes fall much below these calculated for any of the velocity distributions shown in Figure 17, though close to the values for the distribution designated V_2. It should be noted that only seven lattice points are available to describe the different radii of flow, and generally only the outer two lattice points differ significantly from a constant velocity of flow. Hence, the

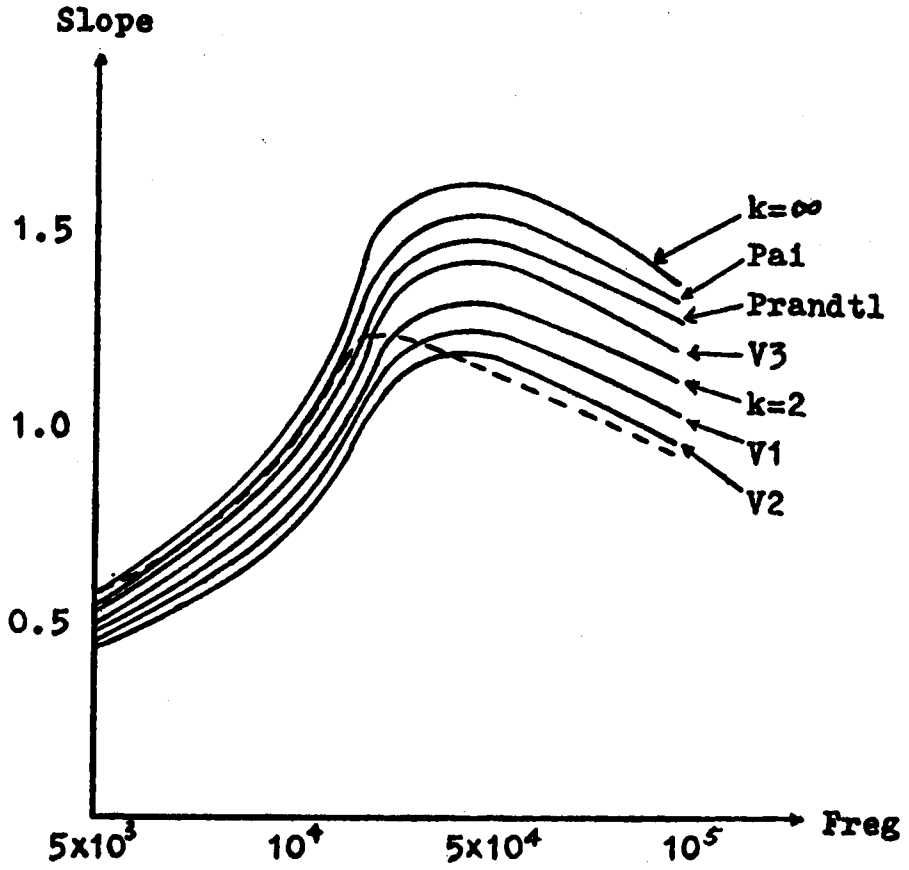


Figure 23. Calculated and measured slopes for various velocity distributions.

coarseness of the relaxation grid severely limits the accuracy with which the pattern and its boundary can be located, and it makes the velocity assumed at the outer two lattice points extremely critical. It is also possible that some systemic error may be responsible for the low empirical data at high frequencies. For purposes of comparison, the plane-wave eddy-current skin depth, $\delta=\sqrt{2/\omega\mu\sigma}$ is about equal to the radius of the tube at 7 KHz for the mercury used in this experiment. Hence, the lowest frequencies (5 KHz) were penetrating deeply into the fluid, whereas the highest frequencies (100 KHz) definitely were not.

Three-Coil System Probe Tube

Using the relaxation method, we have calculated the voltages expected for two different types of three-coil system: An existing coil with two pickup coils located inside the ends of the driver coil as shown in Figure 24, and various configurations of pickup and driver coils with the same radius as shown in the top part of Figure 8 (page 33). The results of the calculations for the former system with constant velocity profile and the experimental data obtained using it with mercury as the flowing fluid are shown in Figure 25. Since the voltage calculated or measured for both three-coil systems were much smaller than those calculated and measured for the five-coil system, it was not analyzed further.

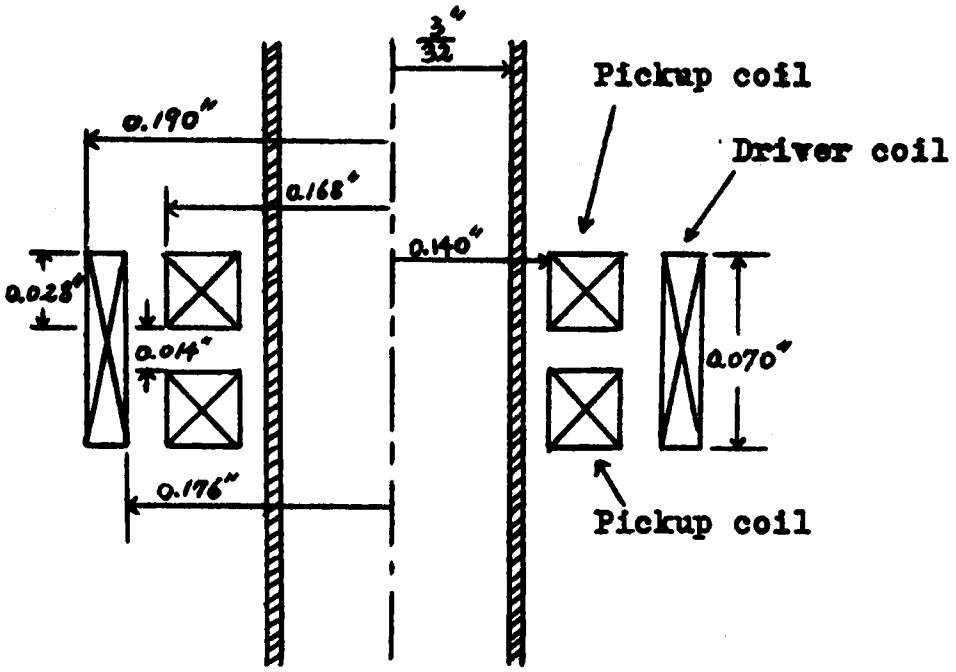


Figure 24. Diagram of the existing three-coil system.

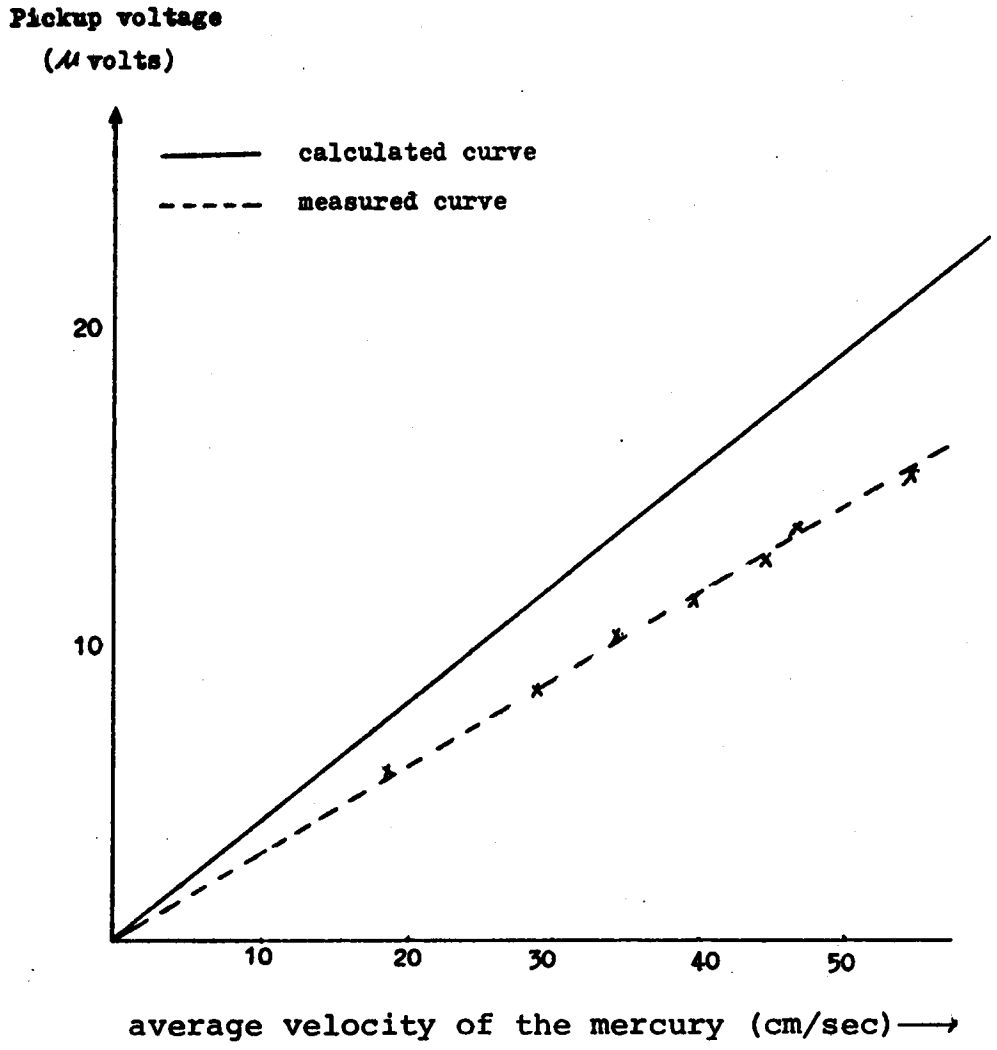


Figure 25. Comparison of the calculated and measured induced voltage of three-coil system probe tube at the frequency of 100 KHz.

Discussion of Errors

The largest percentage error in the calculation is probably due to the coarseness of the relaxation grid. The vector potential is greatly affected by the spacing between the pickup coils and the flowing fluid, while only seven lattice points are available to describe the different radii of flow, and generally only the outer two lattice points affect the vector potential significantly. The error due to the lack of convergence of the vector potential is very small, since the vector potential takes about 500 iterations to converge within 0.001 percent. The error due to geometrical inaccuracy is also very small. We constructed the tube and coils so that their dimensions can be exactly represented by an integral number of lattice points, so the errors are reduced to a minimum.

Other experimental errors are due to the temperature variations of the coils, bubbles in the flowing fluid and electronic noise. The temperature variations of the coils cause changes in coil impedance and coupling between adjacent coils. These effects and the bubbles cause some error in the output pickup voltages. At high frequencies the noise was large enough to make the experimental measurements very difficult, so the accuracy is limited. However, the measurements of the pickup voltages were repeated 10 times at each

velocity and each frequency, and the standard deviations from the mean are less than 5 percent of the mean.

CHAPTER 6

CONCLUSIONS

We have calculated the velocity-dependent voltages developed in several arrangements of flowmeter coils and optimized the spacings and shapes of the coils, as well as the frequency of operation. We have made experimental measurements with an optimized coil system and found the measurements to agree with the calculations for a constant velocity distribution at low frequencies and to agree fairly well at higher frequencies with a modified turbulent flow velocity distribution having a rather thin boundary layer.

It is possible to measure the velocity of a moving conductor quite accurately with encircling eddy-current coils. For solid rods, the operating frequency can be quite high, but for conducting fluids, the operating frequency must be kept low enough that the eddy-currents can penetrate into the fluid to depths where the velocity is reasonably large. However, a suitable frequency analysis can provide much information about the flow velocity as a function of the depth into the fluid, particularly in the boundary region, but limited by the coarseness of the relaxation grid.

BIBLIOGRAPHY

BIBLIOGRAPHY

1. Hughes, D. E. Phil. Mag. 8 (5), 50 (1879).

2. Förster, Friedrich. Z. Metallk. 43, 163-171 (1952).

3. Waidelich, D. L., and C. J. Renken. Proc. Natl. Electron. Conf. 12, 188-196 (1956).

4. Hochschild, R. "Electromagnetic Methods of Testing Metals," Progress in Nondestructive Testing, Vol. 1 (Macmillan Company, New York, 1959).

5. Dodd, C. V., and W. E. Deeds. "Eddy Current Impedance Calculated by a Relaxation Method," pp. 300-314 in Proceedings of the Symposium on Physics and Nondestructive Testing, (Southwest Research Institute, San Antonio, Texas, 1963).

6. Dodd, C. V. A Solution to Electromagnetic Induction Problems, Oak Ridge National Laboratory, ORNL-TM-1802 (1967),, and Ph.D. Dissertation, The University of Tennessee, 1967.

7. Dodd, C. V., and W. E. Deeds. "Electromagnetic Forces in Conductors," J. Appl. Phys. 38 5045 (1967).

8. Dodd, C. V., and W. E. Deeds. "Analytical Solutions to Eddy-Current Probe-Coil Problems," J. Appl. Phys. 39 2829 (1968).

9. Tunstall, J. N., and C. V. Dodd. "A Computer Program to Solve Eddy-Current Problems," Oak Ridge National Laboratory Report K-1740, 1968.

10. Libby, H. L., and J. D. Jensen. "Feasibility Study of Probe-Type Liquid Metal Flowmeters for FTR Subassemblies," Battelle Pacific Northwest Laboratory, BNWL-911, 1969.

11. Klyuev, V. V., M. L. Faingoiz, and G. G. Kapelin. "Movement of a Current-Conducting Plate Parallel to the Plane of a Striding-Type Transducer," The Soviet Journal of Nondestructive Testing, July-August, 1970.

12. Sheff, J. R., and D. L. Lessor. Battelle Pacific Northwest Laboratory, BNWL-SA-4236 (1972).

13. Panofsky, W. K. H., and M. Phillips. Classical Electricity and Magnetism, (Addison-Wesley, 1955), P. 148.

14. Prandtl, L. Ergeb. Aerodyn. Versuchanstalt Göttingen 3, 1 (1927).

15. Pai, S.L J. Appl. Mech. 20, 109 (1953).

APPENDIXES

APPENDIX A

CODE LISTING

```
C ***** EDDY *****

C *** MAIN CONTROL DECK ***
      COMMON//CA(120,54),MATNO(120,54),MAXCT,KOUT,EPS,EPSI,
      RELAX,
     1 SUMA,FMU,PER(16),VCN(16),IZERO(16),VTHETA(16),MM,NN,
     2 NREGA,TOTMAT,AIRMAX,SUMA3,SUMA4
      COMMON/LIMITS/NNDIM,MMDIM
      COMPLEX CA
      INTEGER TOTMAT
      REAL RA(120,54)
      EQUIVALENCE (RA,CA)
C ***INITIALIZE***
      NNDIM=120
      MMDIM=54
      DO 1 M=1,54
      DO 1 N=1,120
    1 CA(N,M)=(0.0,0.0)
      READ(5,8000)NOPT
 8000 FORMAT(15)
C ***AIR CASE***
   10 READ(5,8010)MAXCT,KOUT,EPS,RELAX
 8010 FORMAT(2I5,2F10.5)
      WRITE(6,8020)NOPT,MAXCT,KOUT,EPS,RELAX
 8020 FORMAT(20H1AIR CASE WITH NOPT=,I1/11HOTO BE RUN,15,2X,
    1 26HMAX.  ITERATIONS WITH KOUT=,15,2X,4HEPS=,E15.7,2X,
    2 20HAND WITH RELAXATION=,F10.5)
     CALL GEOM(1)
     CALL AIRVP
     GO TO(50,30),NOPT
C ***CONDUCTOR CASES***
   30 CALL CNVERT
   40 READ(5,8030)EPS,EPSI
 8030 FORMAT(2F10.5)
      WRITE(6,8040)EPS,EPSI
 8040 FORMAT(19H1CONDUCTOR CASES.../10HOWITH EPS=,E17.8,2X,
     1 5HEPSI=,E17.8)
      CALL GEOM (2)
      CALL CONDVP
   50 RETURN
      END
```

```
      SUBROUTINE GEOM(INDEX)
      COMMON//CA(120,54),MATNO(120,54),MAXCT,KOUT,EPS,EPSI,
      RELAX,
     1 SUMA,FMU,PER(16),VCN(16),IZERO(16),VTHETA(16),MM,NN,
     2 NREGA,TOTMAT,AIRMAX,SUMA3,SUMA4
      COMMON/LIMITS/NNDIM,MMDIM
      COMPLEX CA
      INTEGER TOTMAT
      DATA IFLAG1,1FLAG2/-1,-2/
      GO TO(1,100),INDEX
    1 READ(5,8000)NREGA,NN,MM
 8000 FORMAT(3I5)
      IF(NN.GT.NNDIM) GO TO 5
      IF(MM.LE.MMDIM) GO TO 10
    5 WRITE(6,8010)NN,MM
 8010 FORMAT(11H1EITHER NN=,13,7H or MM=,I3,5H EXCEEDS ITS
     1ALLOWABLE  LIMIT..  OPERATION TERMINATED.)
      CALL INPUT(NREGA)
      CALL MESH(IFLAG1)
      CALL OUTPUT(1)
      RETURN
  100 READ(5,8000)NCDTOR
      CALL INPUT(NCDTOR)
      CALL MESH(IFLAG2)
      TOTMAT=NREGA+NCDTOR
      CALL OUTPUT(2)
      RETURN
      END

      SUBROUTINE INPUT(K)
      COMMON//CA(120,54),MATNO(120,54),MAXCT,KOUT,EPS,EPSI,
      RELAX,
     1 SUMA,FMU,PER(16),VCN(16),IZERO(16),VTHETA(16),MM,NN,
     2 NREGA,TOTMAT,AIRMAX,SUMA3,SUMA4
      COMPLEX CA
C ****THIS ROUTINE READS PROPERTIES FOR K MATERIALS.
      DO 10 L=1,K
   10 READ(5,8000)IMAT,PER(IMAT),VCN(IMAT),IZERO(IMAT),
      VTHETA(IMAT)
 8000 FORMAT(I2,3X,2F10.5,3X,I2,F8.5)
      IF((VCN(IMAT)*FLOAT(IZERO(IMAT))).EQ.0) GO TO 20
      WRITE(6,8010)IMAT,PER(IMAT),VCN(IMAT),IZERO(IMAT),
      VTHETA(IMAT)
 8010 FORMAT(21H1THE MATERIAL INDEXED,I2,11H WHERE PER=,E15.7,
      5H VCN=,
     1 E15.7,11H AND IZERO=,I2,7HVTHETA=,I2/' IS NOT ALLOWABLE.
     2 OPERATION TERMINATED.')
   20 CONTINUE
      RETURN
      END
```

```
      SUBROUTINE MESH(IFLG)
      COMMON//CA(120,54),MATNO(120,54),MAXCT,KOUT,EPS,EPSI,
      RELAX,
     1 SUMA,FMU,PER(16),VCN(16),IZERO(16),VTHETA(16),MM,NN,
     2 NREGA,TOTMAT,AIRMAX,SUMA3,SUMA4
      COMPLEX CA
C ****THIS ROUTINE READS THE RECTANGULAR BOUNDS OF THE
C REGIONS THAT APPROXIMATES THE MATERIALS AND SETS UP THE
C MESH.
   10 READ(5,8000)IMAT,NLG,NUG,MLG,MUG
 8000 FORMAT(I2,3X,4I5)
      IF(IMAT.EQ.IFLG) GO TO 30
      DO 20 N=NLG,NUG
      DO 20 M=MLG,MUG
   20 MATNO(N,M)=IMAT
      GO TO 10
   30 RETURN
      END

      SUBROUTINE OUTPUT(JNT)
      COMMON//CA(120,54),MATNO(120,54),MAXCT,KOUT,EPS,EPSI,
      RELAX,
     1 SUMA,FMU,PER(16),VCN(16),IZERO(16),VTHETA(16),MM,NN,
     2 NREGA,TOTMAT,AIRMAX,SUMA3,SUMA4
      COMPLEX CA
      INTEGER TOTMAT
      GO TO(10,20),JNT
   10 WRITE(6,8000)
 8000 FORMAT(32H1A MAP OF THE AIR CASE GEOMETRY //)
      LASTR=NREGA
      GO TO 30
   20 WRITE(6,8010)
 8010 FORMAT(38H1A MAP OF THE CONDUCTOR CASE GEOMETRY //)
      LASTR=TOTMAT
   30 DO 40 N=1,NN
      N1=(NN+1)-N
   40 WRITE(6,8020)(MATNO(N1,M),M=1,MM)
 8020 FORMAT(1H,54I2)
      WRITE(6,8030)
 8030 FORMAT(33HO WITH THE FOLLOWING PROPERTIES.../8HOMAP
      NO.,2X,
     1 21HRELATIVE PERMEABILITY,2X,12H FMU WEIGHT ,2X,
     2 14HCURRENT SWITCH,2X,15HVELOCITY SWITCH)
      WRITE(6,8040)I,PER(I),VCN(I),IZERO*I),VTHETA(I),I=1,
      LASTR)
 8040 FORMAT(1H ,3X,I2,5X,F12.6,11X,F12.6,9X,I2,16X,F8.5)
      RETURN
      END
```

```
      SUBROUTINE AIRVP
      COMMON//CA(120,54),MATNO(120,54),MAXCT,KOUT,EPS,EPSI,
      RELAX,
     1 SUMA,FUM,PER(16),VCN(16),IZERO(16),VTHETA(16),MM,NN,
     2 NREGA,TOTMAT,AIRMAX,SUMA3,SUMA4
      COMPLEX CA
      REAL RA(120,54)
      EQUIVALENCE (RA,CA)
      DATA TIP/6.2831853/
      MMM=MM-1
      NNN=NN-1
      KOUNTA=0
      OLSUM2=0.0
      OLSUM3=0.0
      OLSUM4=0.0
      WRITE(6,8000)
 8000 FORMAT(49HOSUM OVER THE COIL PER ITERATION FOR AIR
      CASE....)
   10 SUMA3=0.0
      SUMA4=0.0
      SUMA2=0.0
      DO 20 M=2,MMM
      R=M-1
      RINV=1./R
      GAM=1.+RINV
      PSI=1.+GAM+RINV*RINV
      DO 20 N=2,NNN
      K=MATNO(N,M)
      K1=MATNO(N,M+1)
      K2=MATNO(N+1,M)
      VPER=PER(k)
      CURI=IZERO(K)
      ALPHA=VPER/PER(K1)
      BETA=VPER/PER(K2)
      RA(N,M)=RA(N,M)+RELAX*((GAM*ALPHA*RA(N,M+1)+RA(N,M-1)+
     1 BETA*RA(N+1,M)+RA(N-1,M)+VPER*CURI)/(PSI+ALPHA+BETA)
     2 -RA(N,M))
      IF(K.EQ.2) SUMA2=SUMA2+TPI*R*RA(N,M)
      IF(K.EQ.3) SUMA3=SUMA3+TPI*R*RA(N,M)
   20 IF(K.EQ.4) SUMA4=SUMA4+TPI*R*RA(N,M)
      KOUNTA=KOUNTA+1
      IF(KOUNTA.LE.KOUT) GO TO 30
      IF(ABS((SUMA3-(LSUM3)/SUMA3).LE.EPS) GO TO 40
   30 IF(KOUNTA.GE.MAXCT) GO TO 50
      OLSUM2=SUMA2
      OLSUM3=SUMA3
      OLSUM4=SUMA4
      WRITE(6,8010)KOUNTA,SUMA3,SUMA4,SUMA2
```

```
 8010 FORMAT(1H ,I4,4X,E17.9,2X,E17.9,2X,E17.9)
      GO TO 10
   40 WRITE(6,8020)KOUNTA,SUMA3,SUMA4,SUMA2
 8020 FORMAT(23HOCONVERGENCE FOR AIR IN,I6,2X,10HITERATIONS,
      2X,
     1 14HSUM OVER COIL=,E17.9,4X,#17.9,4X,E17.9)
      GO TO 60
   50 WRITE(6,8010)KOUNTA,SUMA3,SUMA4,SUMA2
      WRITE(6,8030)
 8030 FORMAT(35HOITERATION COUNTER EXCEEDED FOR AIR)
C ****CALCULATE AIRMAX****
   60 AIRMAX = 0.
      DO 70 N=1,NN
      DO 70 M=1,MM
   70 IF(RA(N,M).GT.AIRMAX) AIRMAX=RA(N,M)
      WRITE(6,8040) AIRMAX
 8040 FORMAT(37HOTHE MAXIMUM VECTOR POTENTIAL IN AIR=,E17.9)
      RETURN
      END

      SUBROUTINE CONDVP
      COMMON//CA(120,54),MATNO(120,54),MAXCT,KOUT,EPS,EPSI,
      RELAX,
     1 SUMA,FMU,PER(16),VCN(16),IZERO(16),VTHETA(16),MM,NN,
     2 NREGA,TOTMAT,AIRMAX,SUMA3,SUMA4
      COMPLEX CA
      INTEGER TOTMAT
      REAL RA(120,54)
      EQUIVALENCE (RA,CA)
      COMPLEX OLSUM3,OLSUM4,OLSUM2,SUMC2,SUMC3,SUMC4,ZI,E,
      ZN,ZN3,
     1 ZN4,E3,E4,SUMCM,SUMCP,AN
      DATA TPI/6.2831853/
      READ(5,9000)MAXCT,KOUT,FMU,RELAX
 9000 FORMAT(2I5,2F10.5)
      WRITE(6,9010)FMU,RELAX,MAXCT,KOUT
 9010 FORMAT(22H1CONDUCTOR CASE...FMU=,F10.5,2X,11HRELAXATION
      =,F10.5/
     1 7HOMAXCT=,I5,2X,5HKOUT=,I5)
      READ(5,9020)VL
 9020 FORMAT(F12.9)
      MMM=MM-1
      NNN=NN-1
      KOUNT=0
      OLSUM2=(0.0,0.0)
      OLSUM3=(0.0,0.0)
      OLSUM4=(0.0,0.0)
      ZI=(0.0,0.0)
      WRITE(6,8000)
```

```
 8000 FORMAT(55HOSUM OVER THE COIL PER ITERATION FOR THE
     CONDUCTOR CASE)
   10 SUMC3=(0.0,0.0)
      SUMC4=(0.0,0.0)
      SUMC2=(0.0,0.0)
      DO 20 M=2,MMM
      R=M-1
      RINV=1./R
      GAM=1.+RINV
      PSI=1.+GAM+RINV*RINV
      DO 20 N=2,NNN
      K=MATNO(N,M)
      K1=MATNO(N,M+1)
      K2=MATNO(N+1,M)
      THETA=VTHETA(K)
      VPER=PER(K)
      FMUBAR=VCN(K)*FMU
      CURI=IZERO(K)
      ALPHA=VPER/PER(K1)
      BETA=VPER/PER(K2)
      CA(N,M)=CA(N,M)+RELAX*((GAM*ALPHA*CA(N,M+1)+CA(N,M-1)+
     1         (BETA-THETA*VL)*CA(N+1,M)+CA(N-1,M)+VPER*CURI)/
     2         (PSI+ALPHA+BETA-THETA*VL+ZI*FUMBAR)-CA(N,M))
      IF(K.EQ.2) SUMC2=SUMC2+TPI*R*CA(N,M)
      IF(K.EQ.3) SUMC3=SUMC3+TPI*R*CA(N,M)
   20 IF(K.EQ.4) SUMC4=SUMC4+TPI*R*CA(N,M)
      KOUNTC=KOUNTC+1
      IF(KOUNTC.LE.KOUT)GO TO 30
      Z3R=REAL(SUMC3)
      Z3I=AIMAG(SUMC3)
      Z4R=REAL(SUMC4)
      Z4I=AIMAG(SUMC4)
      IF(ABS((Z3R-REAL(OLSUM3))/Z3R).GT.EPS.AND.
     1 ABS((Z4R-REAL(OLSUM4))/Z4R).GT.EPS) GO TO 30
      IF(ABS((Z3I-AIMAG(OLSUM3))/Z3I).LE.EPSI.OR.
     1 ABS((Z4I-AIMAG(OLSUM4))/Z4I).LE.EPSI) GO TO 40
   30 IF(KOUNTC.GE.MAXCT) GO TO 50
      OLSUM2=SUMC2
      OLSUM3=SUMC3
      OLSUM4=SUMC4
      WRITE(6,8010)KOUNTC,SUMC3,SUMC4,SUMC2
 8010 FORMAT(1H ,I4,1X,E17.9,1X,E17.9,1X,E17.9,1X,E17.9,
     1 1X,E17.9,1X,E17.9)
      GO TO 10
C ***CASE CONVERGES***
   40 WRITE(6,8020)KOUNTC,SUMC3,SUMC4,SUMC2
 8020 FORMAT(39HOCONVERGENCE FOR THIS CONDUCTOR CASE IN,I6,2X,
     1 10HITERATIONS/15HOSUM OVER COIL=,E17.9,2X,#17.9,
     2 2X,E17.9,1X,E17.9,2X,E17.9,1X,E17.9)
```

```
      GO TO 60
   50 WRITE(6,8010)KOUNTC,SUMC3,SUMC4,SUMC2
      WRITE(6,8030)
 8030 FORMAT(41HOITERATION COUNTER EXCEEDED FOR THIS CASE)
   60 RETURN
      END

      SUBROUTINE CNVERT
      COMMON//CA(120,54),MATNO(120,54),MAXCT,KOUT,EPS,EPSI,
      RELAX,
     1 SUMA,FMU,PER(16),VCN(16),IZERO(16),VTHETA(16),MM,NN,
     2 NREGA,TOTMAT,AIRMAX,SUMA3,SUMA4
      COMPLEX CA
      REAL RA(120,54)
      EQUIVALENCE (RA,CA)
      DO 10 L1=1,54
      M=55-L1
      DO 10 L2=1,120
      N=121-L2
   10 CA(N,M)=RA(N,M)
      RETURN
      END
```

APPENDIX B

DEFINITION OF PROGRAM VARIABLE

NOPT:	The execution option value.
MAXCT:	The maximum number of iterations to be calculated.
KOUT:	The code executes the first KOUT iterations before testing for convergence.
EPS:	The convergence criteria for real value.
EPSI:	The convergence criteria for imaginary value.
RELAX:	The overrelaxation constant W.
TOTMAT:	The total number of materials, l.
NDCTOR:	The number of conductor materials, c.
NREGA:	The number of materials in the air case, (l-c).
MM:	The number of columns, M, of lattice points.
NN:	The number of rows, N, of lattice points.
CA(N,M):	The complex-valued vector potential, $A_{n,m}$.
RA(N,M):	The real-valued vector potential, $\hat{A}_{n,m}$, calculated in the air case.
MATNO(N,M):	The material index function, $\beta_{n,m,}$ defined Equation (3.12).
VCN(K):	The material index dependent function γ(K) defined in Equation (3.18)

IZERO(K): The material index dependent function $\alpha(K)$ defined in Equation (3.14).

VTHETA(K): The moving conductor dependent function $\theta(K)$ defined in Equation (3.15).

FMU: The value $\hat{F}$ defined in Equation (3.16)

PER(K): The material index dependent function u_k defined in Equation (3.13).

SUMA: The sum over the coil in air case, defined by $2\pi \sum_{\text{coil}} (m-1)\hat{A}_{n,m}$.

SUMC: The sum over the coil in conductor case, defined by $2\pi \sum_{\text{coil}} (m-1)A_{n,m}$.

AIRMAX: The value of max. $\hat{A}_{n,m}$.

IMAT: The variable name used in reading the material index in constructing the geometric configuration.

NLG, NUG, MLG, MUG: The variable name used to construct one rectangle in the geometric configuration.

VL: Defined by: $h\mu\sigma u$,

where h is the distance between two lattice points,

μ is the permeability,

σ is the conductivity,

u is the velocity of the flowing conductor.

APPENDIX C

DESCRIPTION OF CARD INPUT

	Variable Read	Format
Card A:	NOPT	(I5)
Card B:	MAXCT, KOUT, EPS, RELAX:	(2I5,2F10.5)
Card C:	NREGA, NN, MM:	(3I5)
Card D_j:	IMAT, PER(IMAT), VCN(IMAT), IZERO(IMAT), VTHETA(IMAT):	(I2,3X,2F10.5,3X,I2,F8.5)

for $j = 1,2,\ldots\ldots,NREGA$

(Cards D_j defined the functions u_k, $\gamma(K)$, $\alpha(K)$, and $\theta(K)$ for $K = 1,2,\ldots\ldots,NREGA$)

Card E_i: IMAT, NLG, NUG, MLG, MUG: (I2,3X,4I5)

for $i = 1,2,\ldots,p$, where $p = \sum_{k=1}^{NREGA} p_k$

(Each card E_i describes a rectangle, giving the vertex "coordinates" and material index of the points)

Card F: "-1" (I2)

(Card F signals the code that the air case geometry has been defined)

Card G: EPS, EPSI: (2F10.5)

Card H: NCDTOR: (I5)

Card I_j: IMAT, PER(IMAT), VCN(IMAT),

IZERO(IMAT),

(VTHETA(IMAT): (I2,3X,2F10.5,3X,I2,F8.5)

for j = 1,2,....,NCDTOR.

(Cards I_j defined the functions u_k, $\gamma(K)$, $\alpha(K)$, and $\theta(K)$ for K = [NREGA+1],.....,1).

Card J_i: IMAT, NLG, NUG, MLG, MUG: (I2,3X,4I5)

for i = 1,2,.....,Q, where $Q = \sum_{k=NREGA+1}^{1} Q_K$

(Each card J_i describes a rectangle for a conductor material)

Card K: "-2": (I2)

Card L: MAXCT, KOUT, FMU, RELAX: (2I5,2F10.5)

Card M: VL: (F12.8)

APPENDIX D

The following data cards are for the double layer five-coil system, at the frequency of 50 KHz. The velocity profile of the flowing conductor is assumed to be constant at the rate of 20cm/sec. (Table I).

TABLE I

DATA CARDS

	1 . . . 5	6 . . . 10	11 . . . 15	16 . . . 20	21 . . . 25	26 . . . 30	31 . . . 35	36 . . .
Card A	2							
Card B	500	100	.000	01	1.9			
Card C	6	120	54					
Card D_1	1	1.0		0.0		0	0.0	
Card D_2	2	1.0		0.0		-1	0.0	
Card D_3	3	1.0		0.0		0	0.0	
Card D_4	4	1.0		0.0		0	0.0	
Card D_5	5	1.0		0.0		1	0.0	
Card D_6	6	1.0		0.0		-1	0.0	
Card E_1	1	1	120	1	54			
Card E_2	2	75	76	10	11			
Card E_3	3	67	70	10	11			
Card E_4	4	51	54	10	11			
Card E_5	5	59	62	10	11			
Card E_6	6	45	46	10	11			

APPENDIX D (continued)

	1 . . . 5	6 . . . 10	11 . . . 15	16 . . . 20	21 . . . 25	26 . . . 30	31 . . . 35	36 . . .
Card F	-1							
Card G	.0000		.0000	1				
Card H	9							
Card I_1	7	1.0		35.4		0	0.0	
Card I_2	8	1.0		1.0		0	1.0	
Card I_3	9	1.0		1.0		0	1.0	
Card I_4	10	1.0		1.0		0	1.0	
Card I_5	11	1.0		1.0		0	1.0	
Card I_6	12	1.0		1.0		0	1.0	
Card I_7	13	1.0		1.0		0	1.0	
Card I_8	14	1.0		1.0		0	1.0	
Card I_9	15	1.0		1.0		0	1.0	
Card J_1	7	1	3	12	54			
Card J_2	7	118	120	12	54			
Card J_3	7	4	117	52	54			
Card J_4	8	1	120	8	8			
Card J_5	9	1	120	7	7			
Card J_6	10	1	120	6	6			
Card J_7	11	1	120	5	5			
Card J_8	12	1	120	4	4			
Card J_9	13	1	120	3	3			
Card J_{10}	14	1	120	2	2			

APPENDIX D (continued)

	1 . . . 5	6 . . . 10	11 . . . 15	16 . . . 20	21 . . . 25	26 . . . 30	31 . . . 35	36
Card J_{11}	15	1	120	1	1			
Card K	-2							
Card L	1500	100	0.04	992	1.2			
Card M	0.00	00447						

The layout of the problem on a lattice of points is shown in Figure 26.

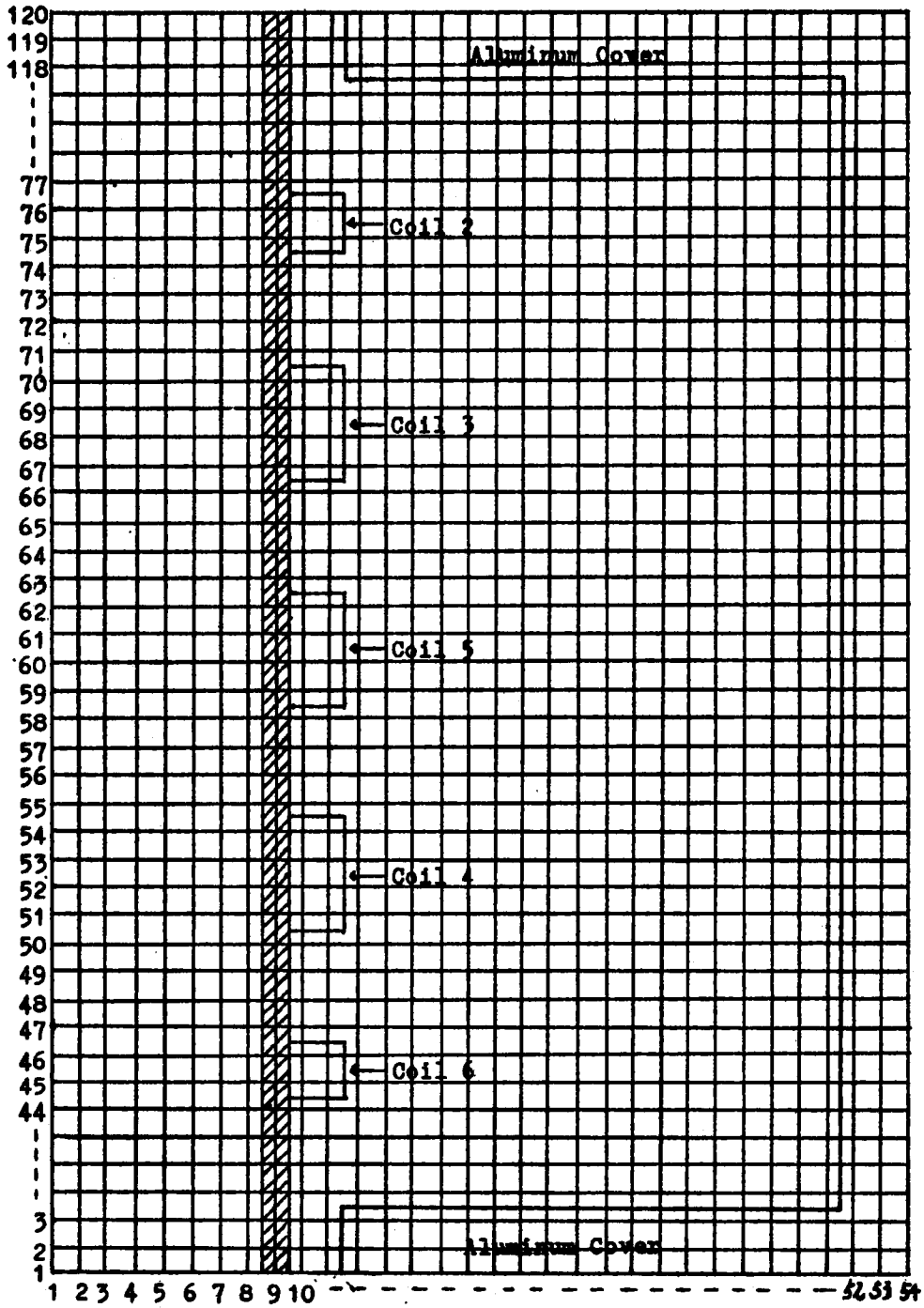


Figure 26. The layout of the double layer five-coil system on a lattice of points.

VITA

The author, Chi-Chau Feng, was born in Hwangpu, Kwantung, China on July 15, 1928. He was graduated from Chinese Naval Academy in 1950. He served with the Chinese Navy from that time until 1963. In September, 1963, he entered the National Central University, Taiwan, majoring in Geophysics, and received his M.S. degree in 1965. In 1966, he entered The University of Tennessee, majoring in Physics, and received another M.S. degree in June, 1968. He had worked for The Institute of Nuclear Energy Research in Taiwan for two years and then returned to The University of Tennessee to continue his Ph.D program and received his Ph.D degree in June, 1975.

He is married to Susanna A. S. Feng at Columbus, Missouri, in December 1967.